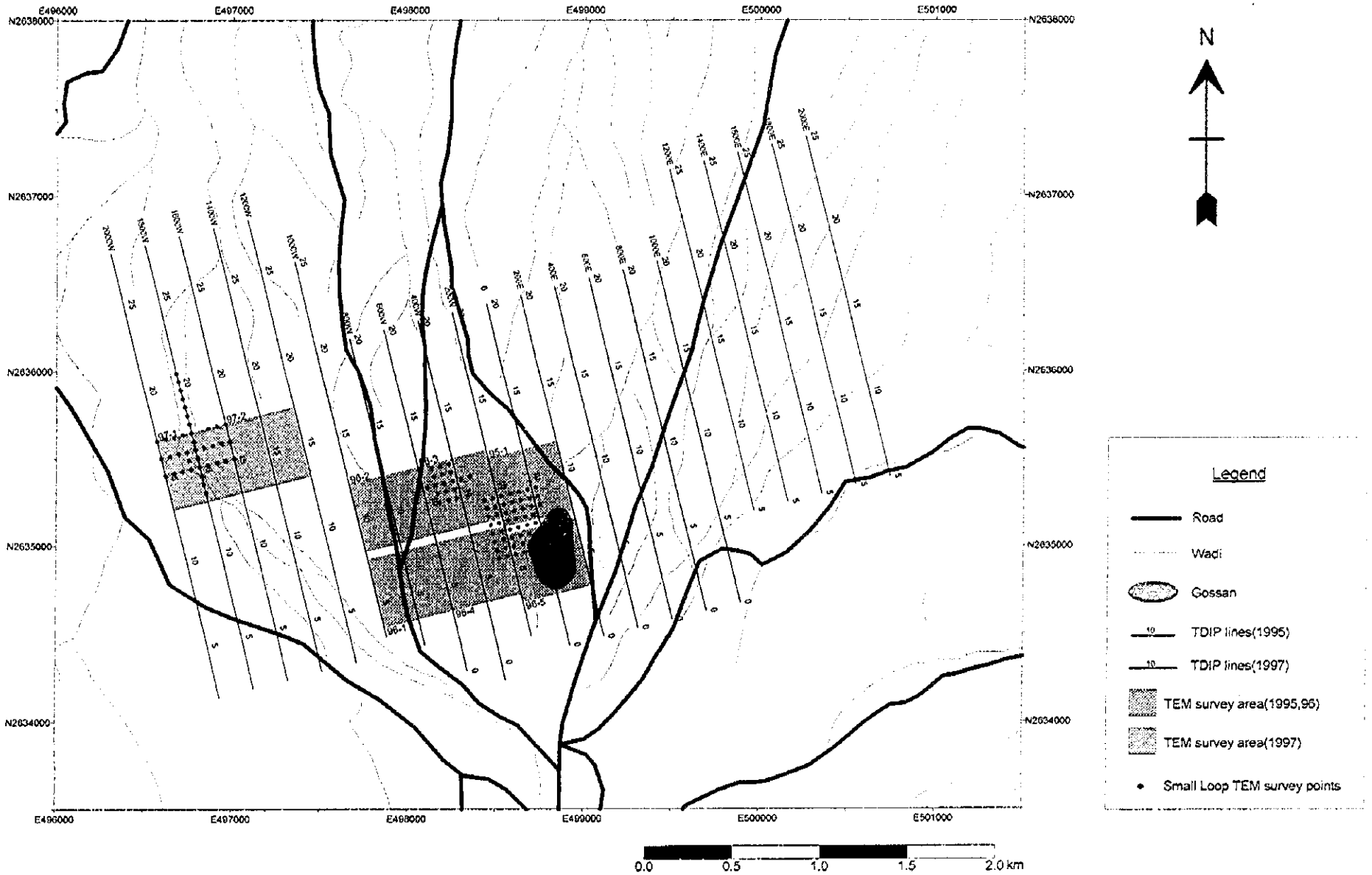

Fig. II -2-4 Geophysical survey location in Ghuzayn area

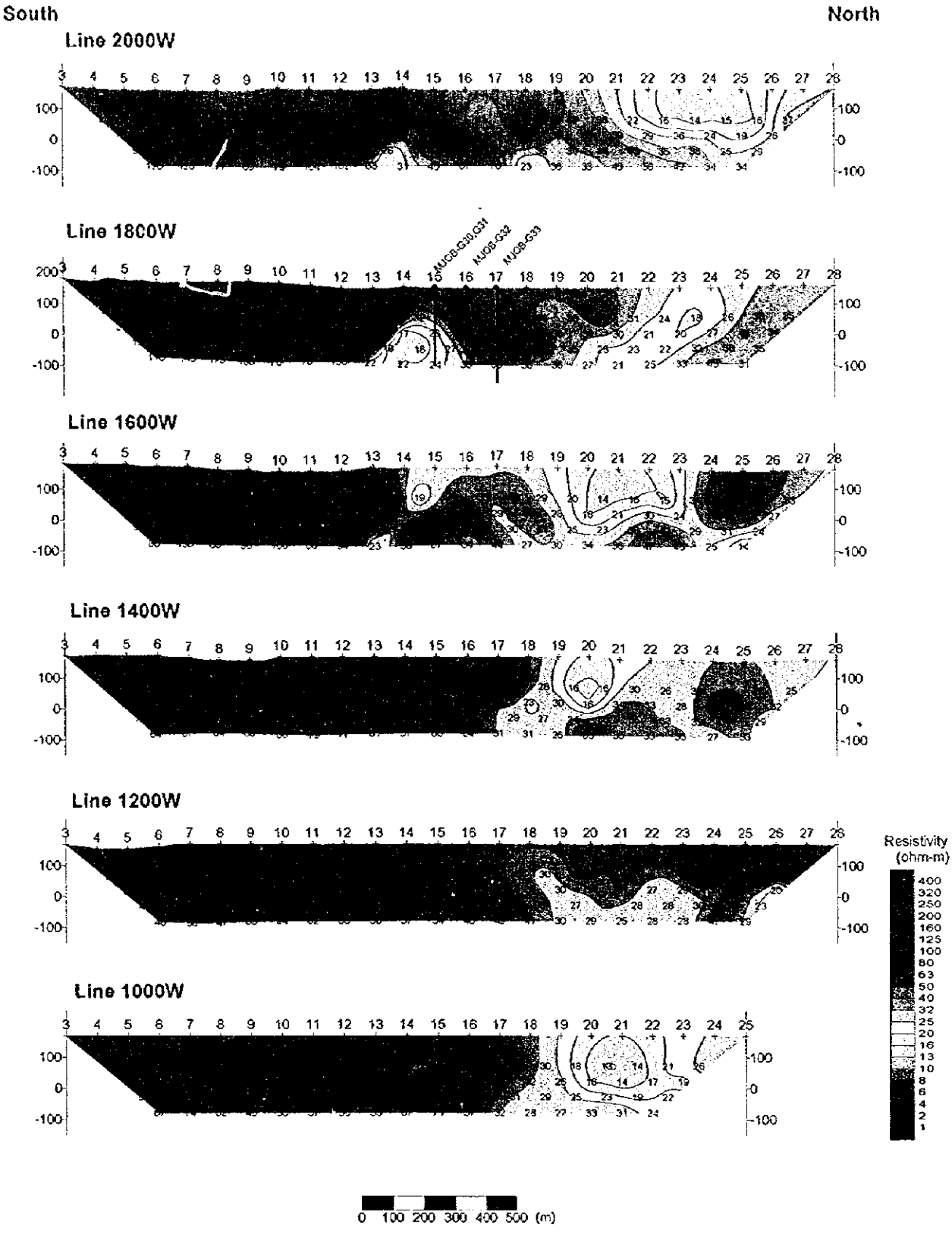

Fig. II -2-5 Apparent resistivity pseudo-sections in Ghuzayn area west side

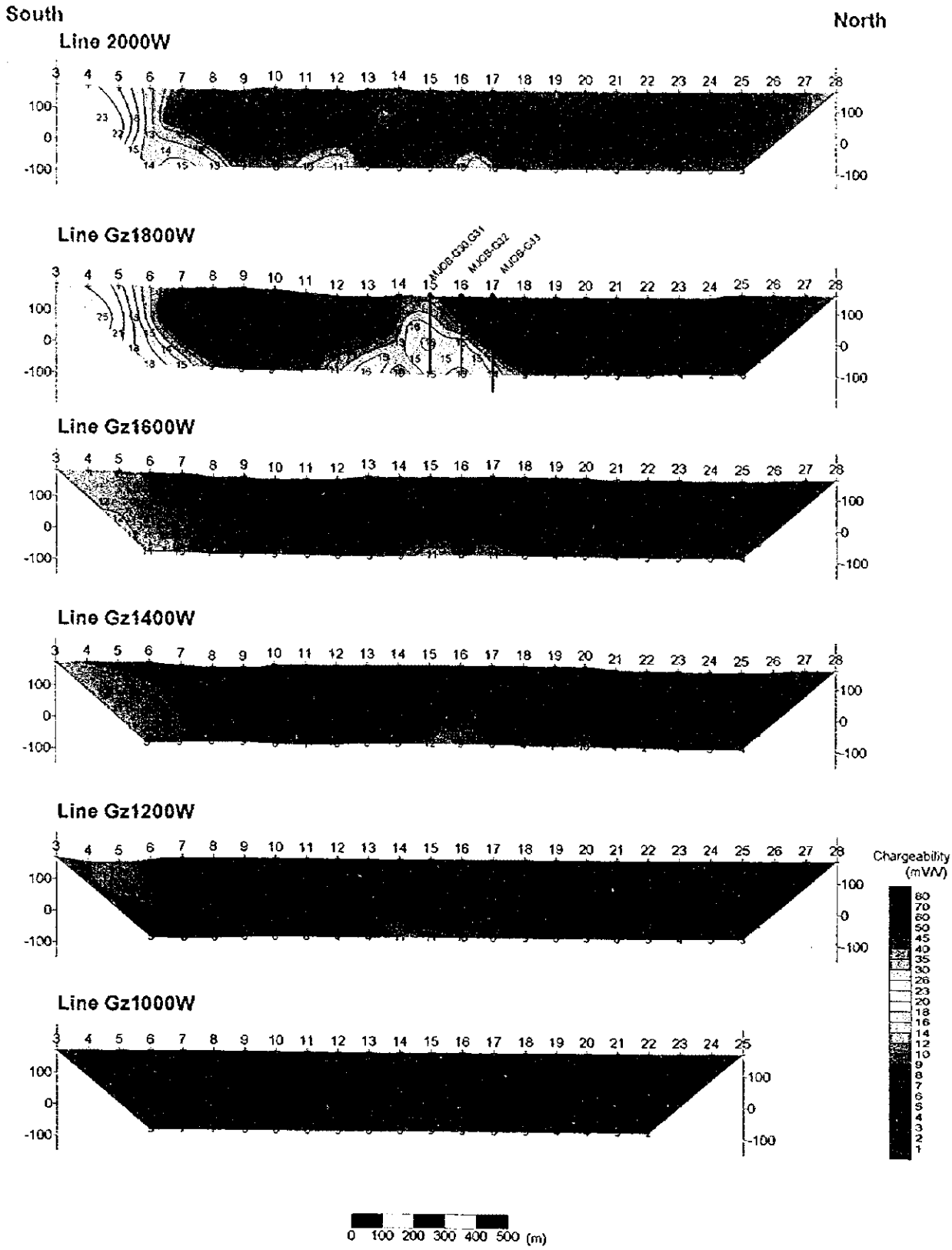

Fig. II -2-6 Chargeability pseudo-sections in Ghuzayn area west side

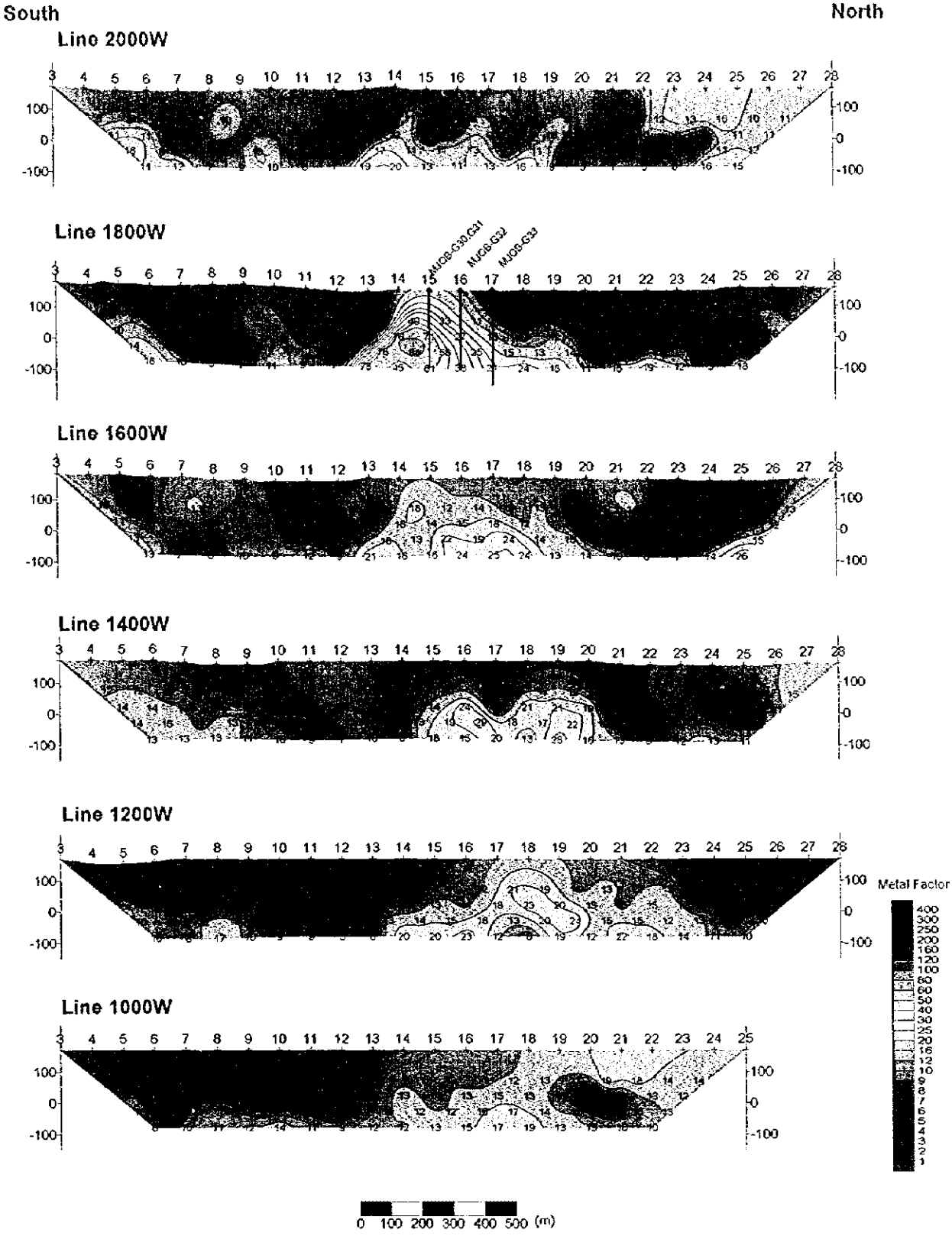

Fig. II-2-7 Metal factor pseudo-sections in Ghuzayn area west side

East Side:

Based on the apparent resistivity contour map indicated in the Fig. II-2-12, it can be seen in the eastern part of this area, a low resistivity distribution in the north part, and a high resistivity distribution of more than 100 Ωm detected towards the south and extended continuously around the gossan in agreement with the results obtained during the 1996 field survey. The inferred boundary between these high and low resistivity zones seems to extend south-eastward from station No. 18 of the line 1200E to the station No. 9 of the line 2000E.

As shown by the chargeability contour map of the above mentioned figure, intermediate chargeability values around 10 mV/V are seen distributed to the south and concordant with the high resistive zone previously mentioned. In the north part of this area, low chargeability values under 5 mV/V are seen distributed (see Fig. II-2-9).

Slightly high metal factor values of about 20 were detected at deep levels (N=3, 4) around station No. 15 of the lines 1200E and 1400E.

Judging from the above mentioned results, the east side of this area are not considered promising for the existence of mineral deposits.

(3) 2D Analysis

Figs. II-2-15 to II-2-17 present the calculated (resistivity, chargeability and metal factor) two-dimensional simulated results for the lines from 1200W to 2000W.

The line 1800W presents special features deserved to be mentioned. On the central part of this line, below station No. 15, resistivities of less than 20 Ωm are interpreted below 100m depth. At deeper depths, the resistivity values become lower. The adjacent lines 1600W and 2000W which also present resistivity values as low as 30 Ωm , can be interpreted as a continuation of the low resistivity distribution detected in the line 1800W. In the north part of the lines 1400W to 2000W low resistivity values between 10 and 20 Ω m are detected.

In relation to the chargeability values, the station No. 15 on the line 1800W shows a circular distribution of about 20mV/V at a depth of about 150m. On the lines 1200W to 1600W, a similar distribution is seen, however, their chargeability values are relatively lower. To the south , the lines 1800W and 2000W present analyzed anomalies of about 25mV/V.

High metal factor values of above 100 are seen in the station No 15 of the line 1800W at depths below 100m and increasing with depth. As same as for the case of the chargeability distributions, the lines 1600W and 2000W adjacent to 1800W present high metal factor values of about 50 below station No 15 at deep levels.

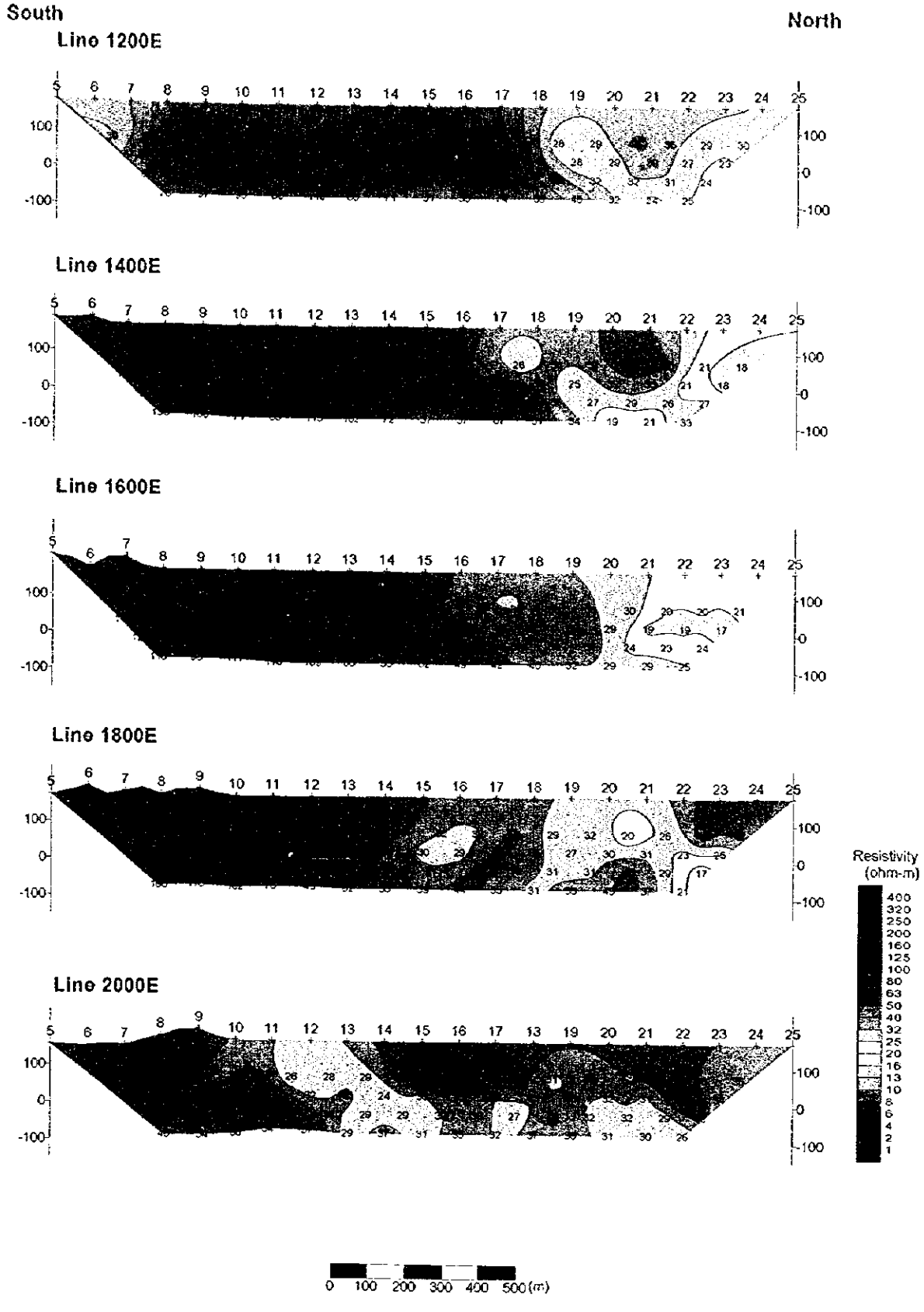

Fig. II -2-8 Apparent resistivity pseudo-sections in Ghuzayn area east side

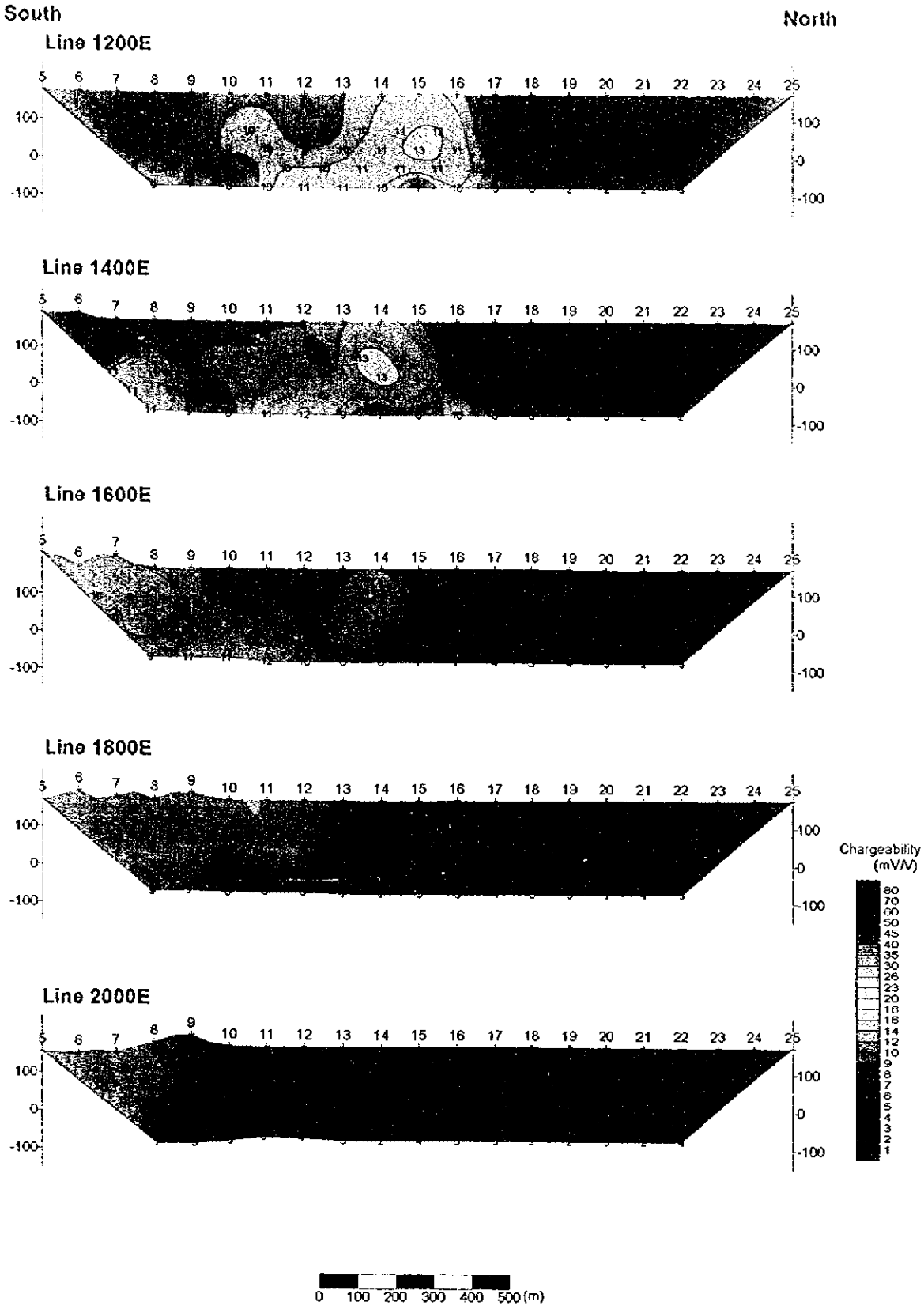

Fig. II -2-9 Chargeability pseudo-sections in Ghuzayn area east side

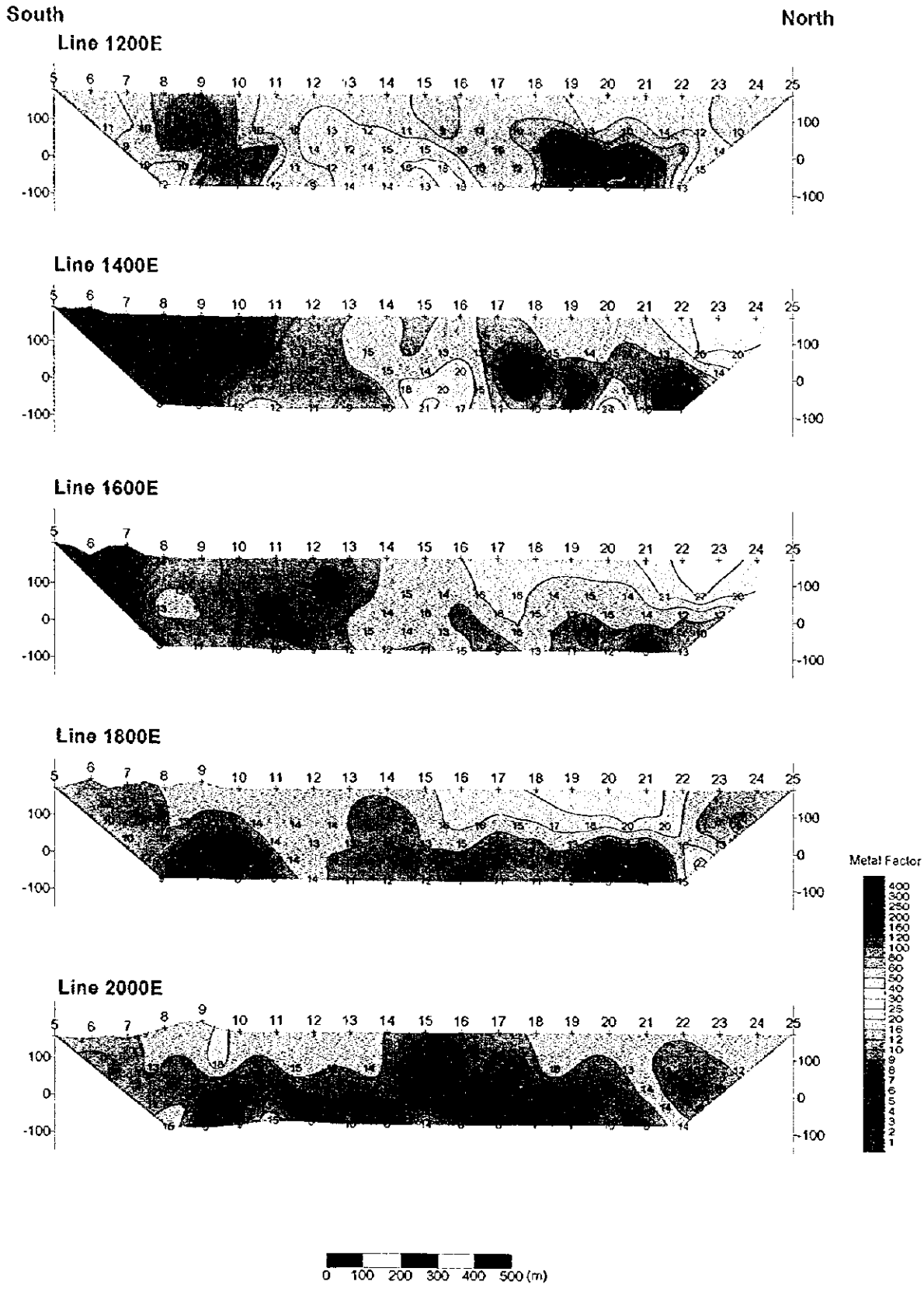

Fig. II -2-10 Metal factor pseudo-sections in Ghuzayn area east side

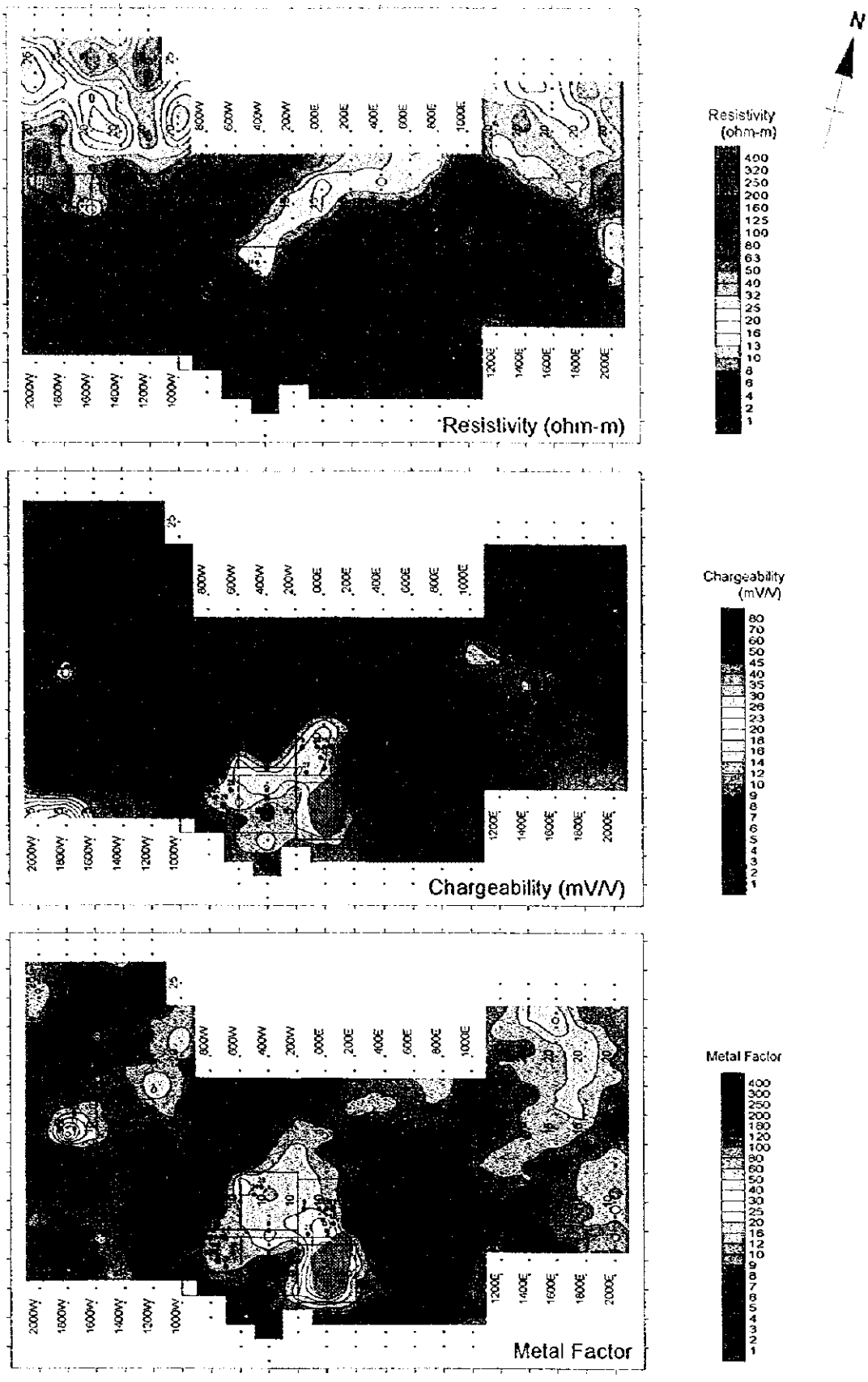

Fig. II -2-11 IP plane map of n=1 in Ghuzayn area

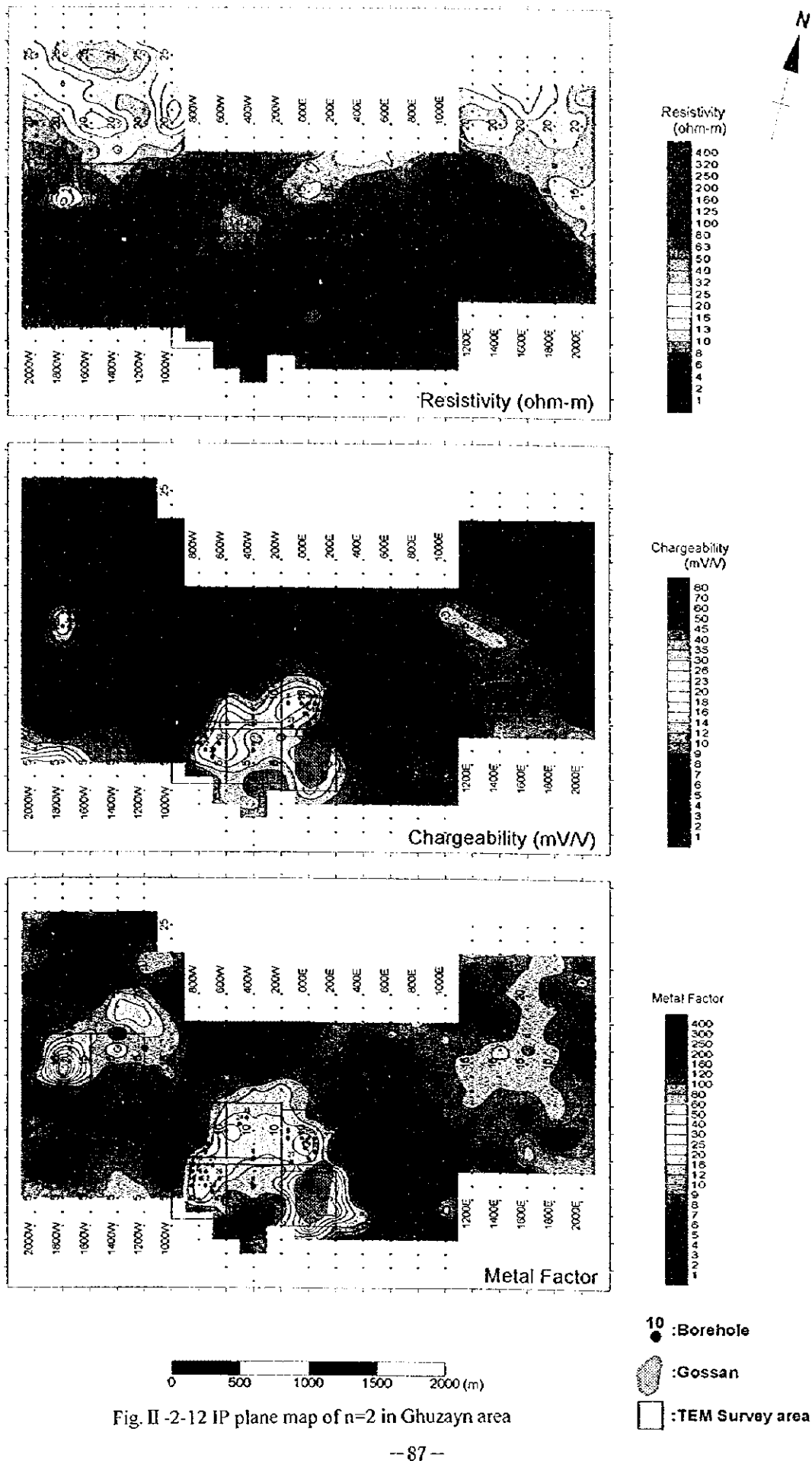

Fig. II -2-12 IP plane map of n=2 in Ghuzayn area

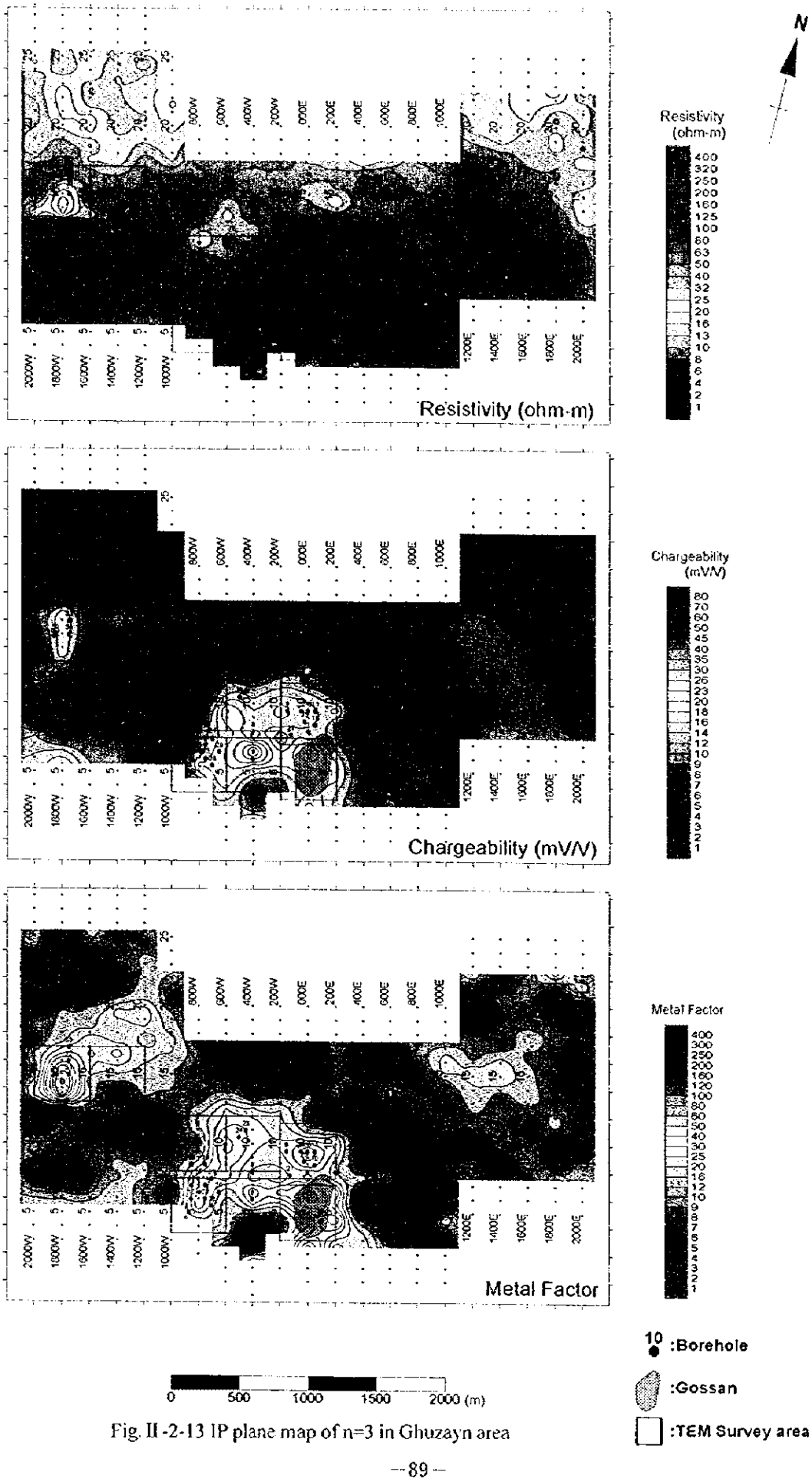

Fig. II-2-13 IP plane map of n=3 in Ghuzayn area

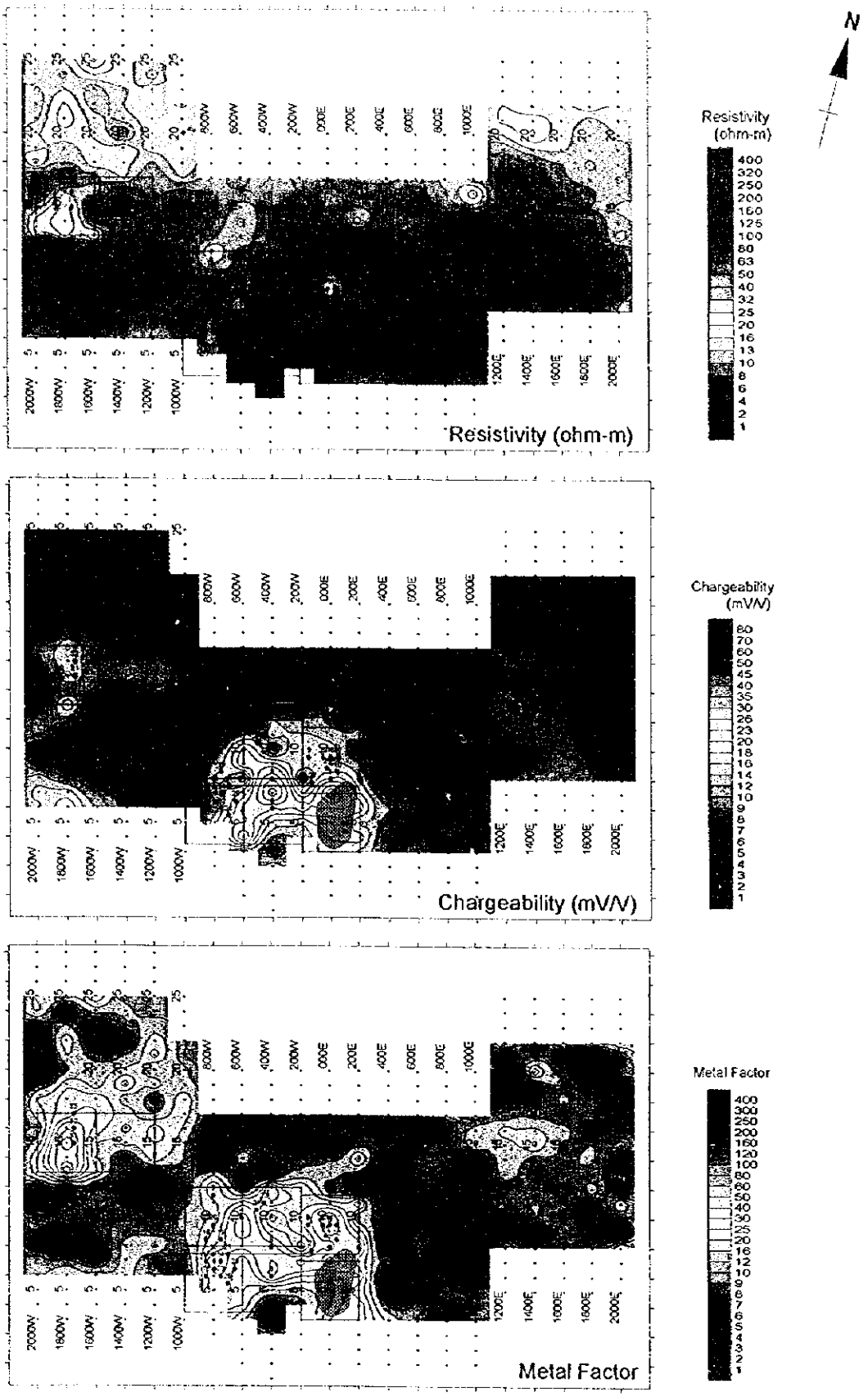

Fig. II -2-14 IP plane map of n=4 in Ghuzayn area

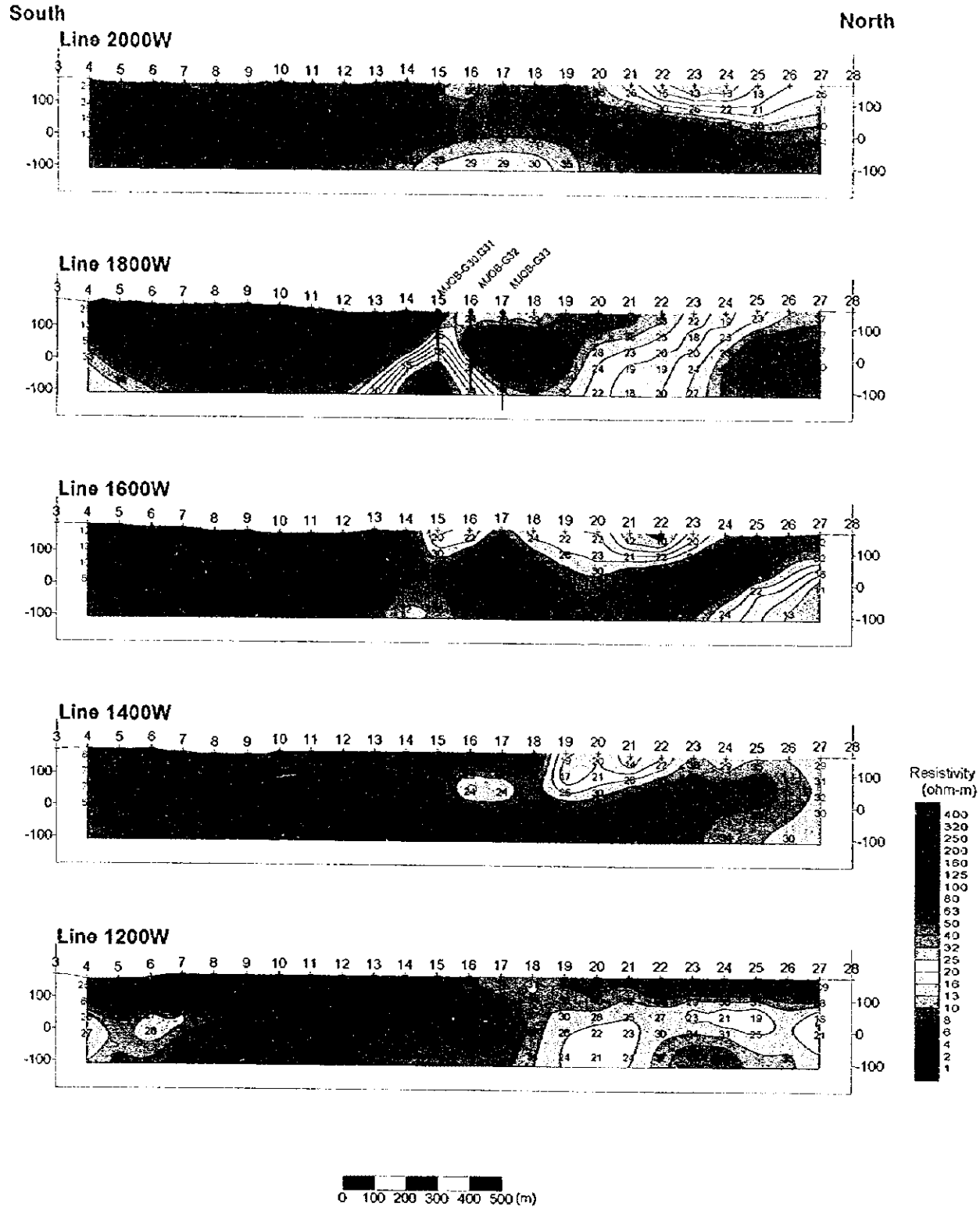

Fig. II -2-15 IP resistivity model simulation on Ghuzayn area west side

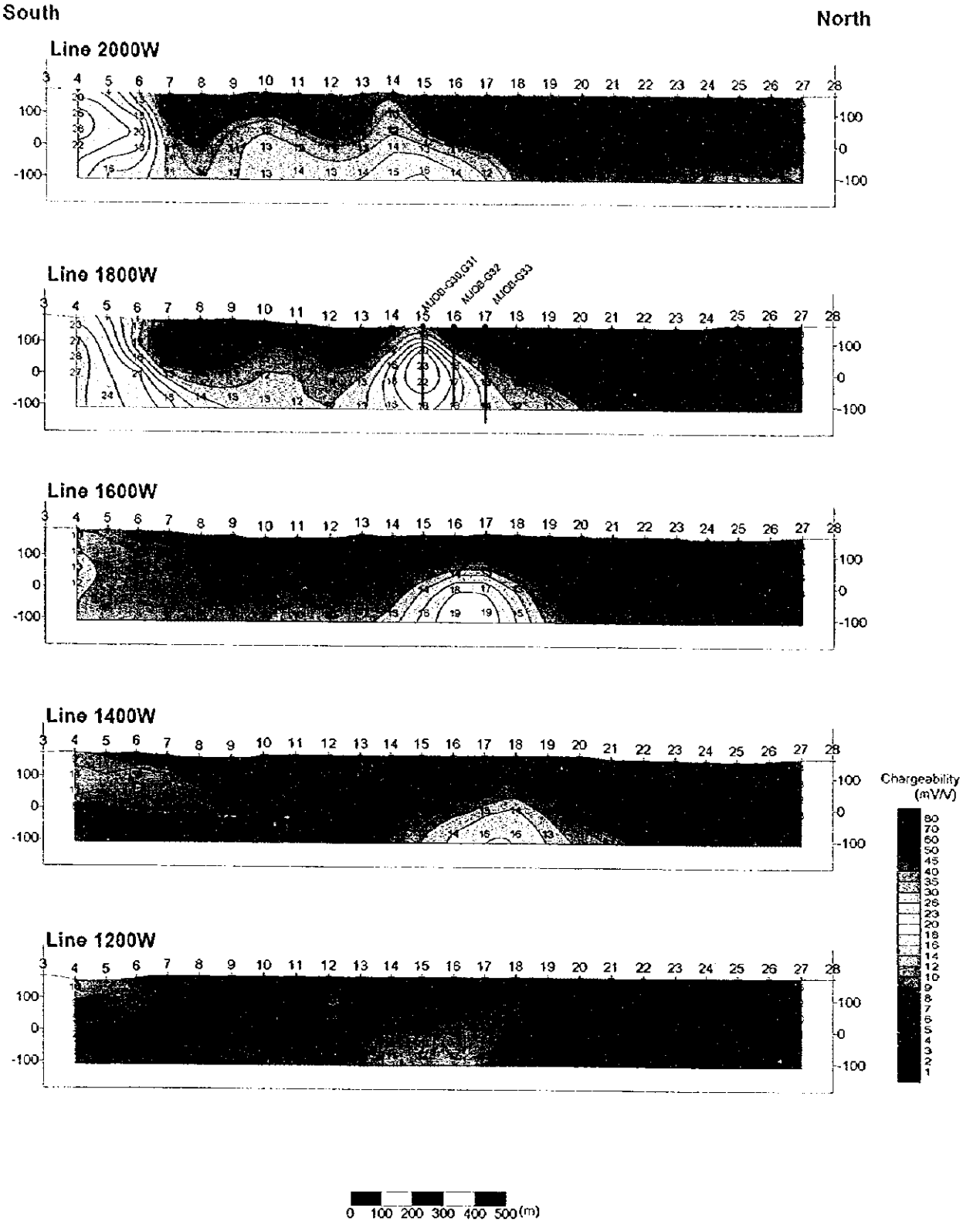

Fig. II -2-16 IP Chargeability model simulation on Ghuzayn area west side

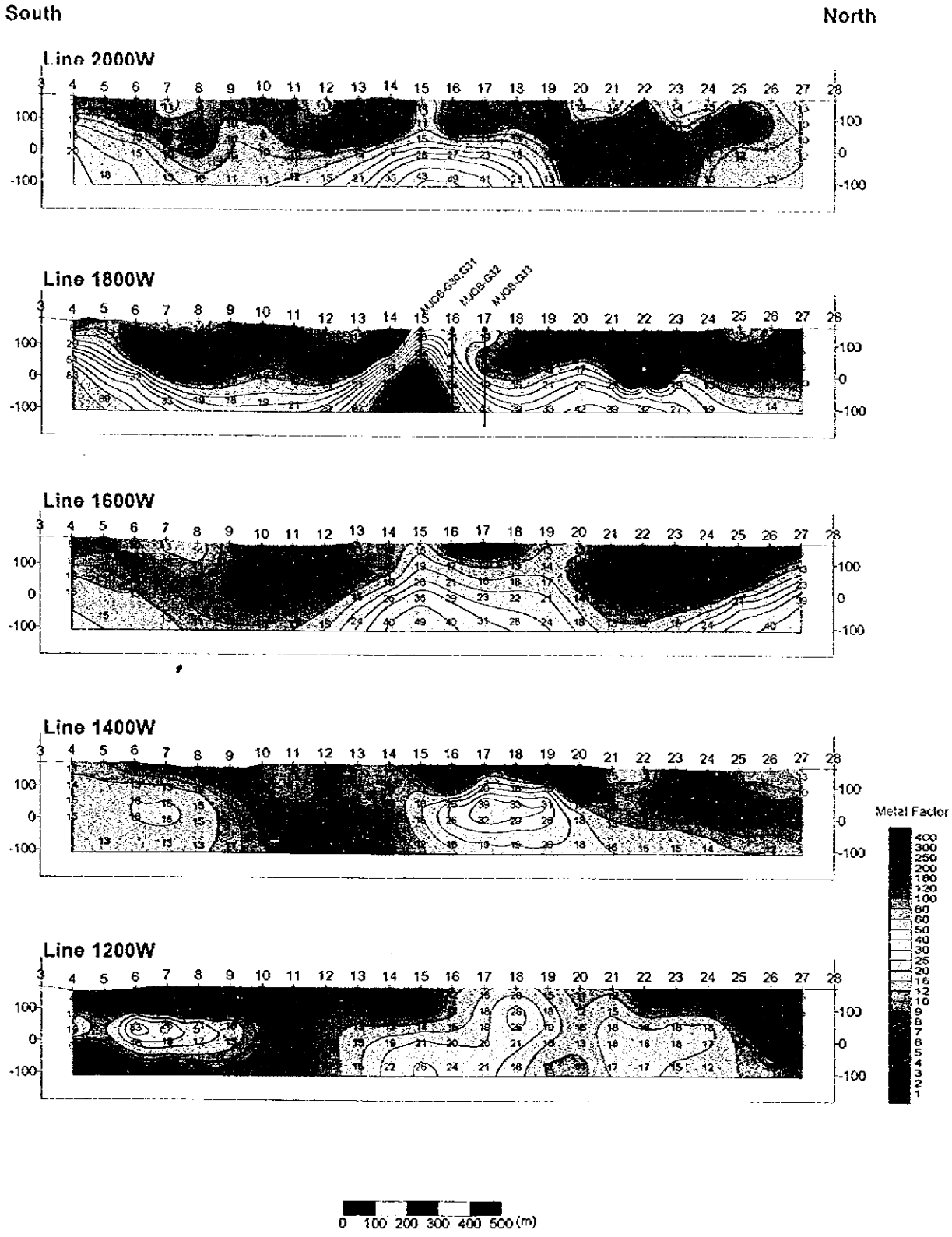

Fig. II -2-17 IP Metal factor model simulation on Ghuzayn area west side

2-5-3 Doqal Area

(1) Lines location

During the 1996 field survey, a total of 7 lines (600N to 600S) of 1.5km each were set along E-W direction. During this phase (1997), the above mentioned lines were extended towards west by 2.0km each. New 3 lines were also added, i.e., two lines (800S and 1000S) of 2.5km each were located to the south of the previous lines and one line (800N) located on the northern side.

The Fig. II-2-18 shows the location of all the IP lines surveyed in Doqal.

(2) Results

The Figs. II-2-19, II-2-20 and II-2-21 show respectively, the compiled pseudo-section results of apparent resistivity, chargeability and metal factor for the 10 lines (added and new) surveyed during the field surveys of 1996 and 1997. Figs. II-2-22, II-2-23, II-2-24 and II-2-25 present the above mentioned results in plane view for N=1 to 4.

In reference to the Fig. II-2-23, the apparent resistivity values are in general low in the north part but high in the south, indicating a transitional discontinuity between the lines 200S and 400S. Furthermore, in the north part a low resistivity distribution of about 10 □m is seen extended southward from the station No. -11 of the line 800N. Also, around station No. -1 in the east side of the same line 800N, another low resistivity distribution is seen to continue as far as the line 400N. An intermediate resistivity distribution of a width of about 400m is seen distributed from the central part of the area towards the line 1000S.

The chargeability results obtained during the 1996 field survey, detected an anomaly distribution of a maximum of about 26mV/V around the gossan zone and extended southward. During the 1997 field survey, the compiled IP results (see Fig. II-2-23) confirmed the extension of the above mentioned distribution towards north-west as far as the station No. -6 of the line 800N, however, its distributed values are less than the distributions around the gossan and with a width of about 200m. This high chargeability distribution becomes smaller towards the north of the line 200S, showing no anomalies from the west side (see Fig.II-2-20(2)) of the gossan. The conspicuous high chargeability distribution is not seen to the south of the line 200S, although maximum values of about 15 mV/V were detected.

Based on the metal factor results, the 1996 field survey detected anomalies in the zones surrounding the gossan. The 1997 field survey confirmed its northwest extension up to the station No. -8 of the line 800N. Southward from the gossan, the metal factor value becomes rather weak (see Figs. II-2-21 and II-2-23).

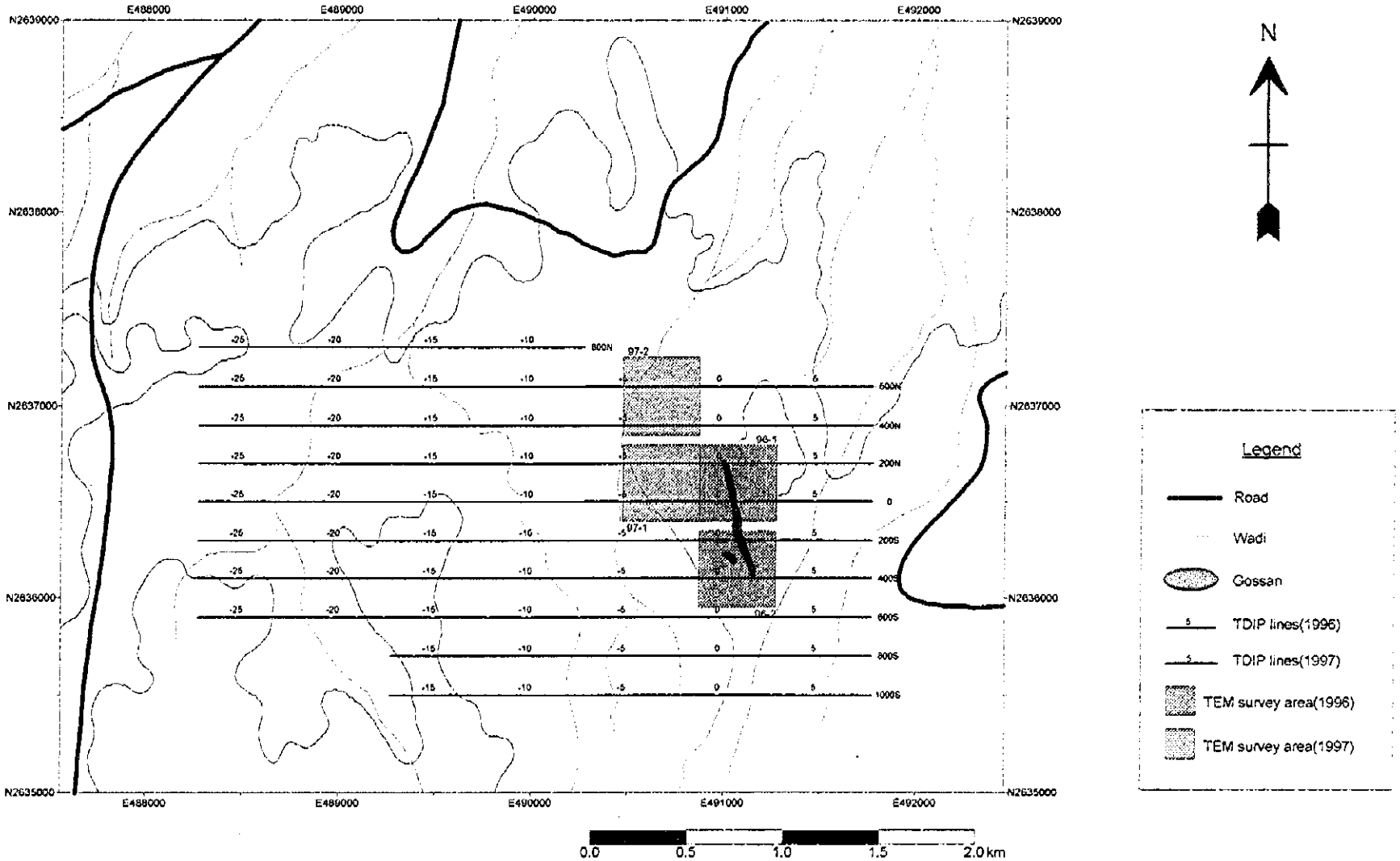

Fig. II-2-18 Geophysical survey location in Doqal area

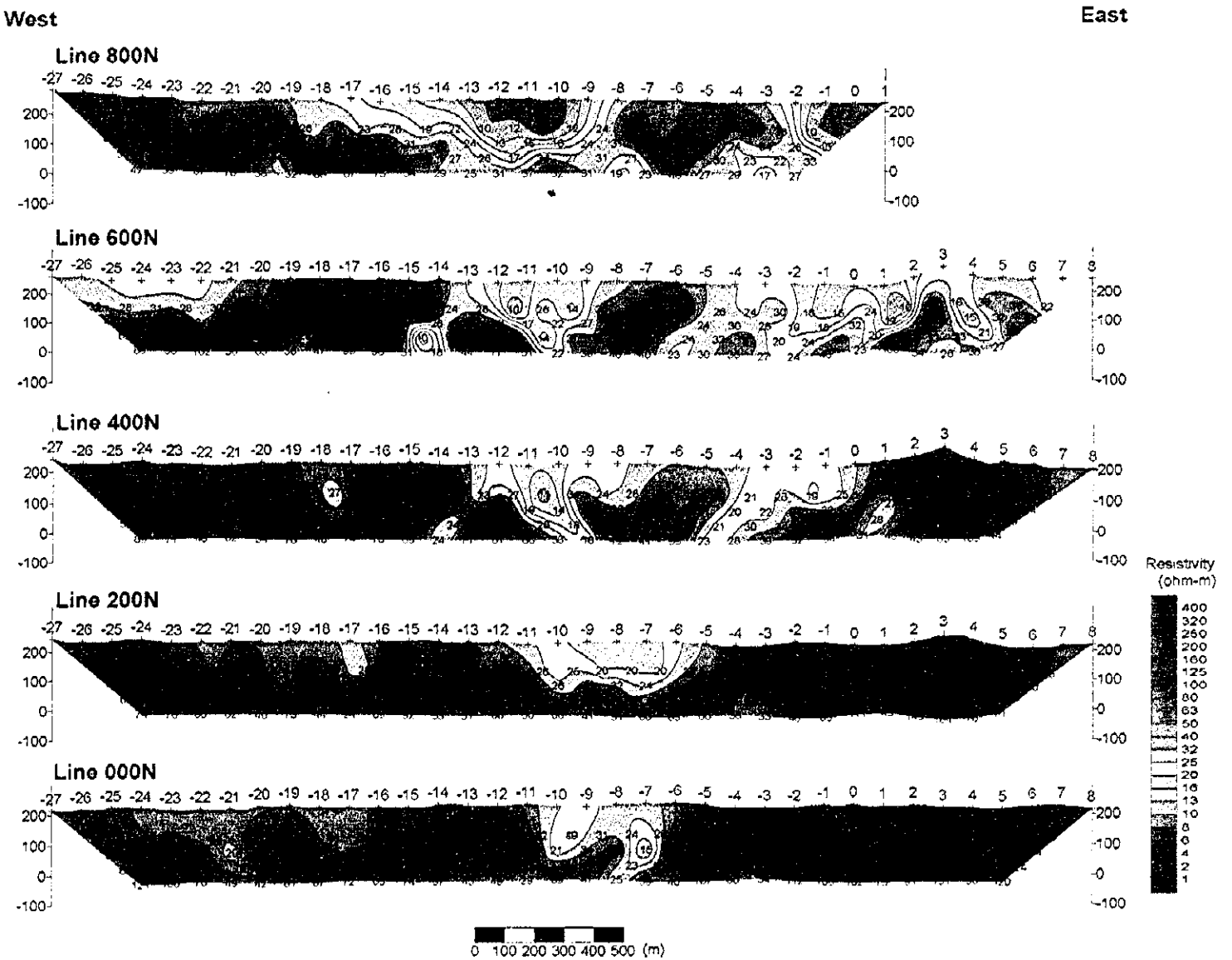

Fig. Ⅱ-2-19(1) Apparent resistivity pseudo-sections in Doqal area

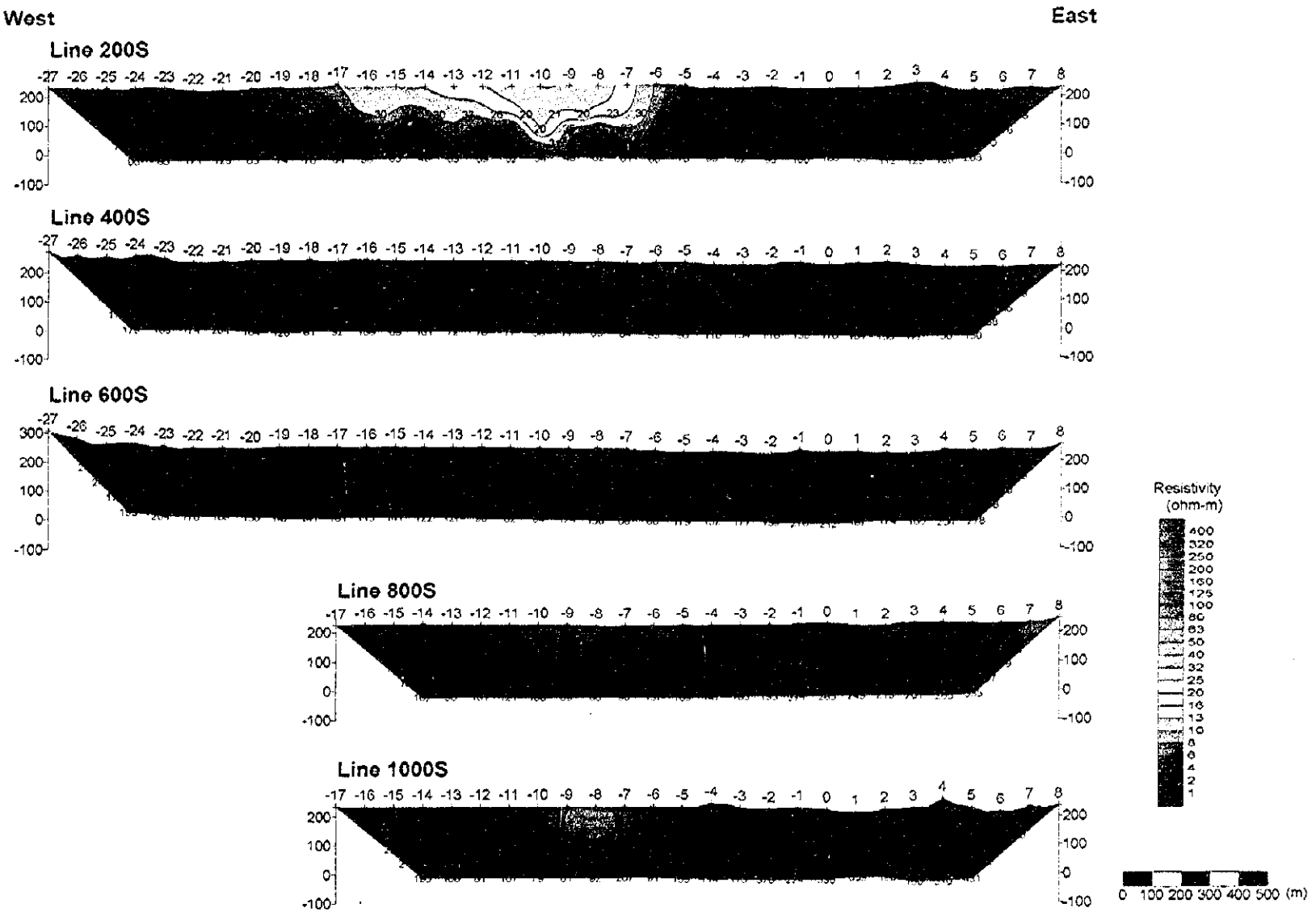

Fig. II-2-19(2) Apparent resistivity pseudo-sections in Doqal area

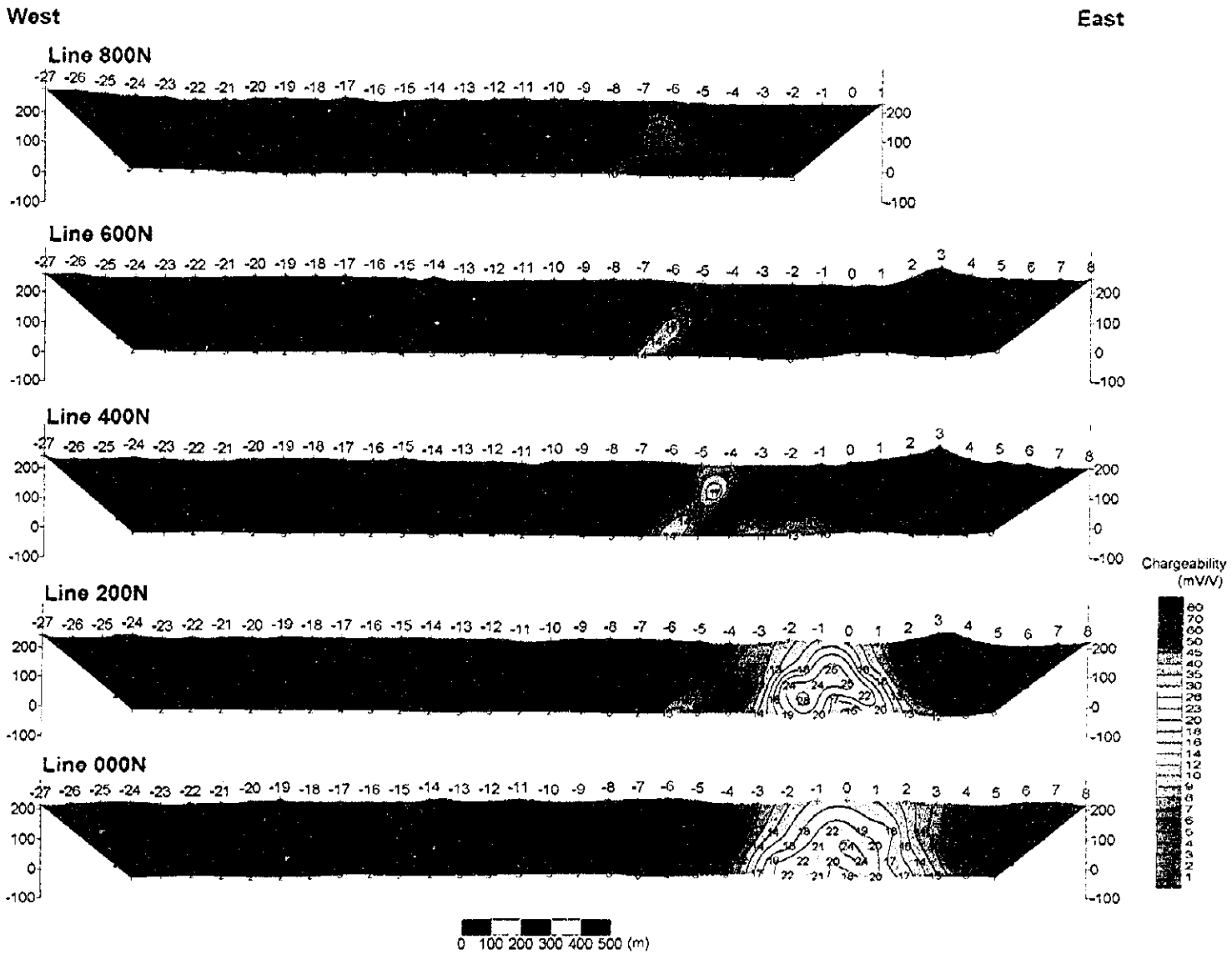

Fig. II -2-20(1) Chargeability pseudo-sections in Doqal area

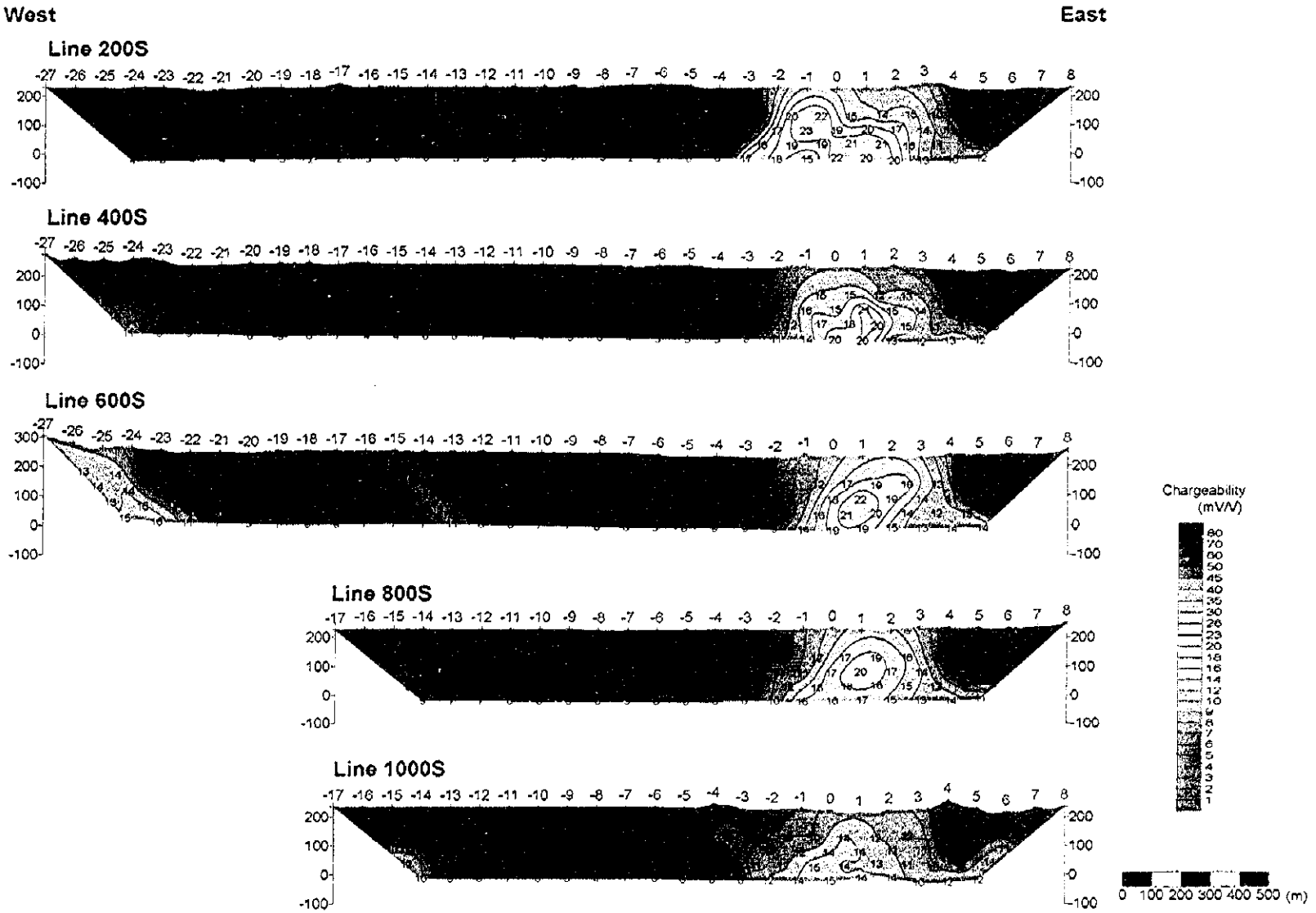

Fig. II-2-20(2) Chargeability pseudo-sections in Doqal area

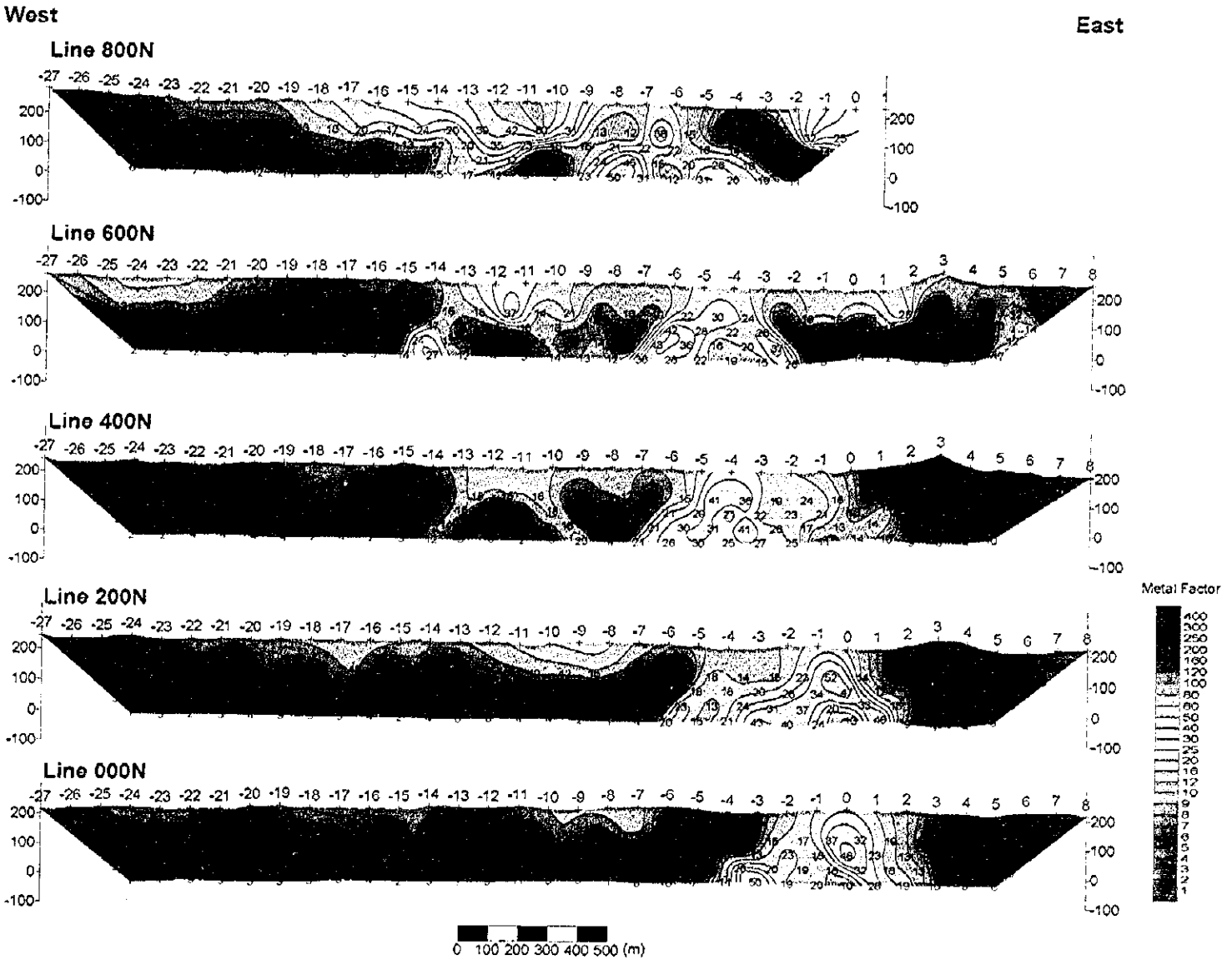

Fig. II-2-21(1) Metal factor pseudo-sections in Doqal area

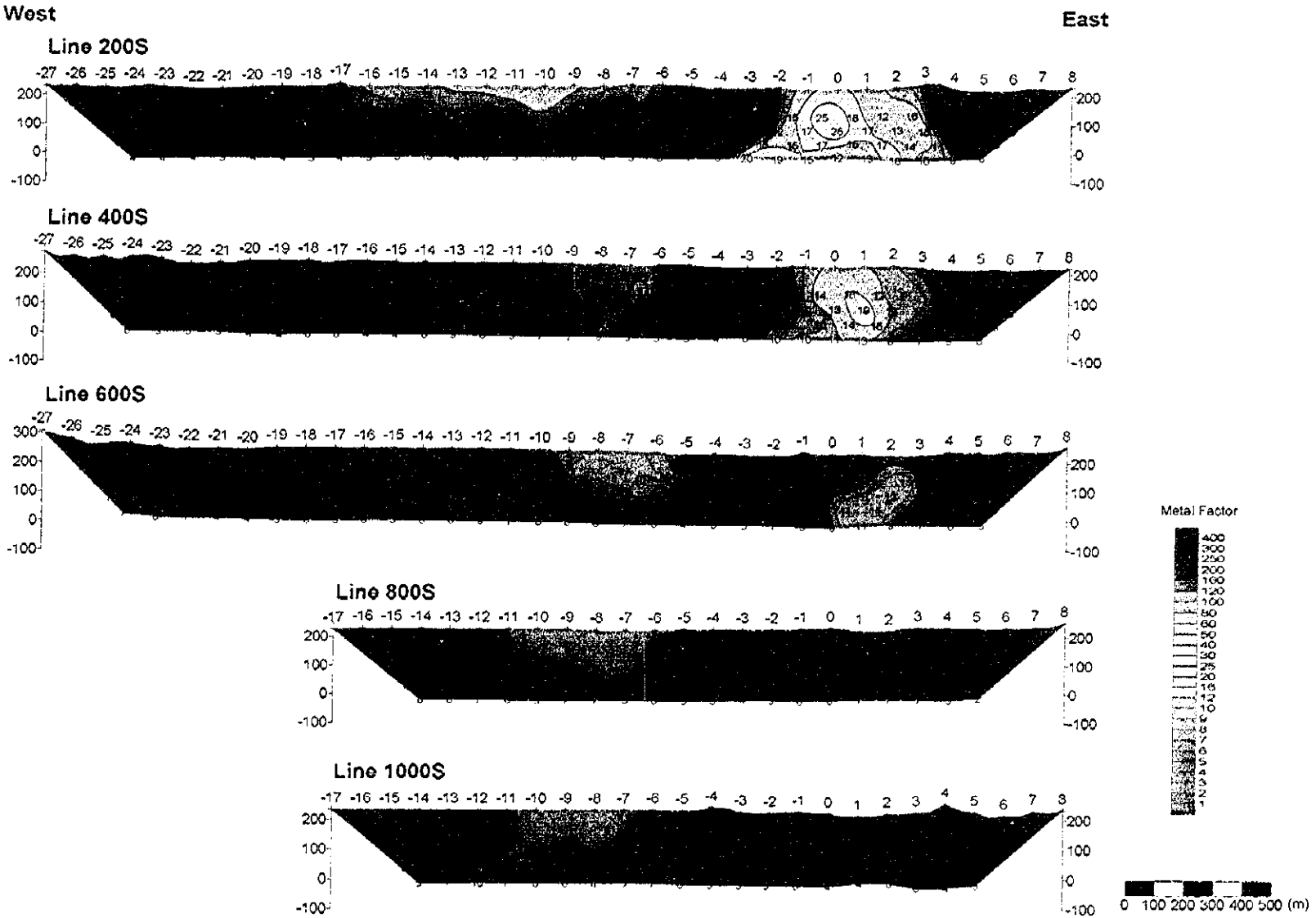

Fig. II -2-21(2) Metal factor pseudo-sections in Doqal area

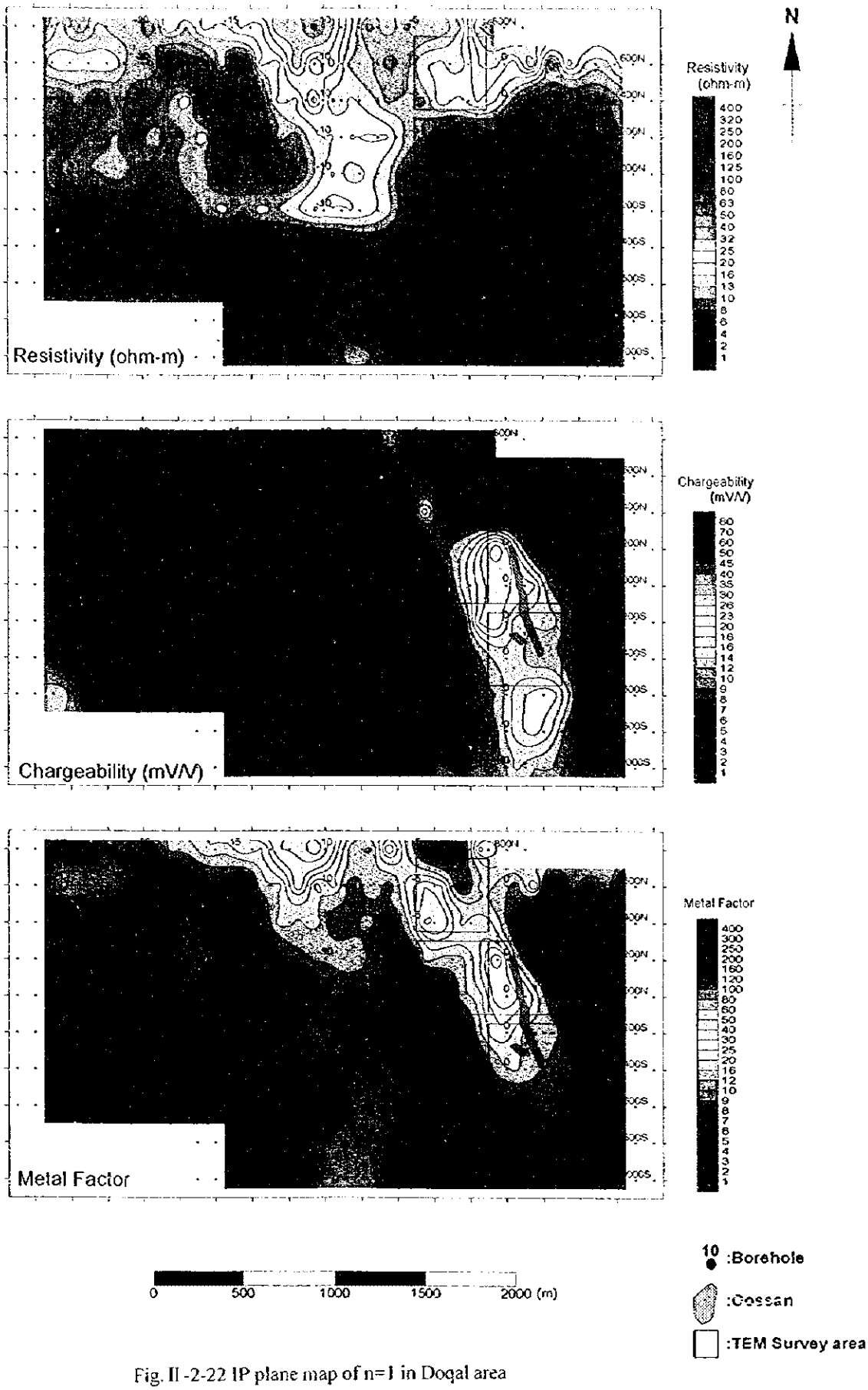

Fig. II -2-22 IP plane map of n=1 in Doqal area

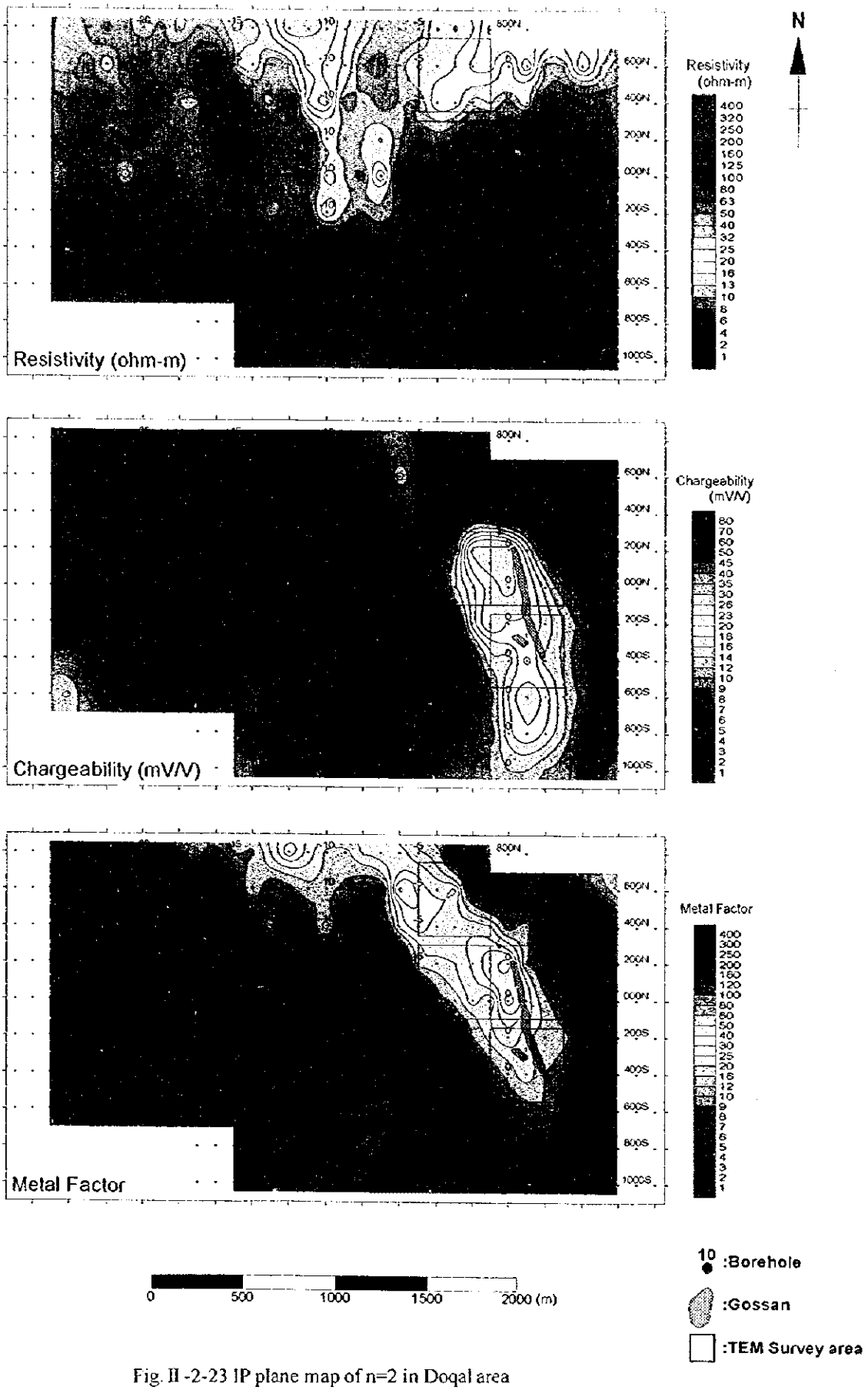

Fig. II -2-23 IP plane map of n=2 in Doqal area

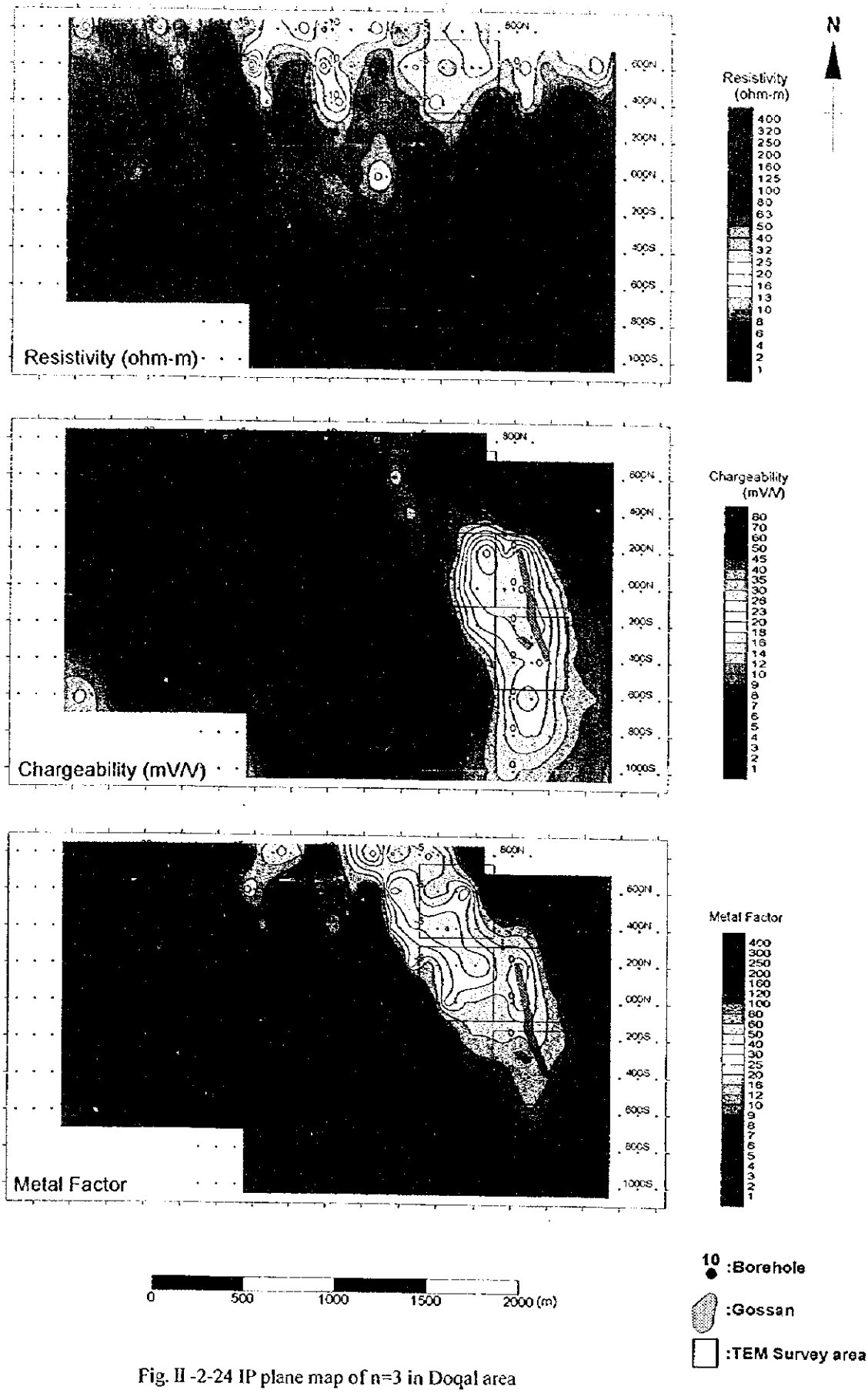

Fig. II -2-24 IP plane map of n=3 in Doqal area

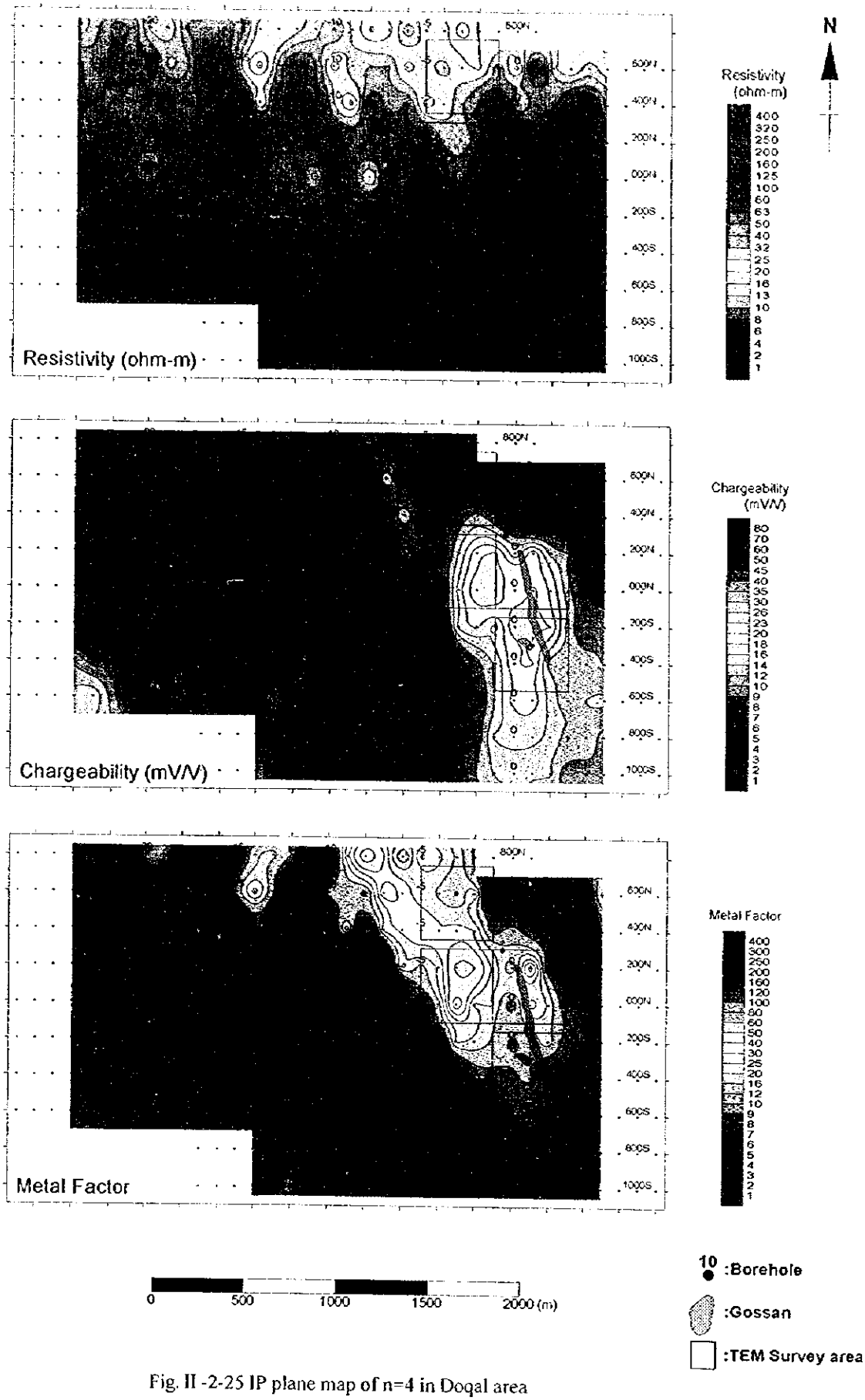

Fig. II -2-25 IP plane map of n=4 in Doqal area

(3) 2-D Analysis

2-D analysis were carried out for all the 10 IP lines. The results of the model calculations are presented here as resistivity sections (Fig. II-2-26), chargeability sections (Fig.II-2-27) and metal factor sections (Fig. II-2-28).

According to the resistivity sections shown in Fig. II-2-26 and which were obtained from the model calculations, it can be inferred that at a depth of about 200m, a low resistivity distribution of about 20 □m can be detected below the station No -5 of the line 800N and extended at depth towards station No -2 of the line 200N. Also on line 800N near the surface below station No -11 as a center, a low resistivity distribution of as low as 10 □m is seen at shallow levels and extended towards line 200S.

Regarding the model results of the chargeability calculations shown in Fig. II-2-27, a remarkable anomaly is seen distributed at certain depth below station No -6 of line 800N and extended to the south as far as the line 1000S. Specially, from line 200N to 400S the anomaly becomes wider, but the scale of this anomaly decreases considerable to the north of line 400N. Furthermore, from 400S to 100S and to the west of the above mentioned anomalies, several weak anomaly distributions are interpreted.

The metal factor calculations displayed in Fig. II-2-28, indicate almost same pattern as that explained for the chargeability sections. According to these calculations, it is only seen a remarkable anomaly which extends from 800N below station No -6 towards south (line 800S).

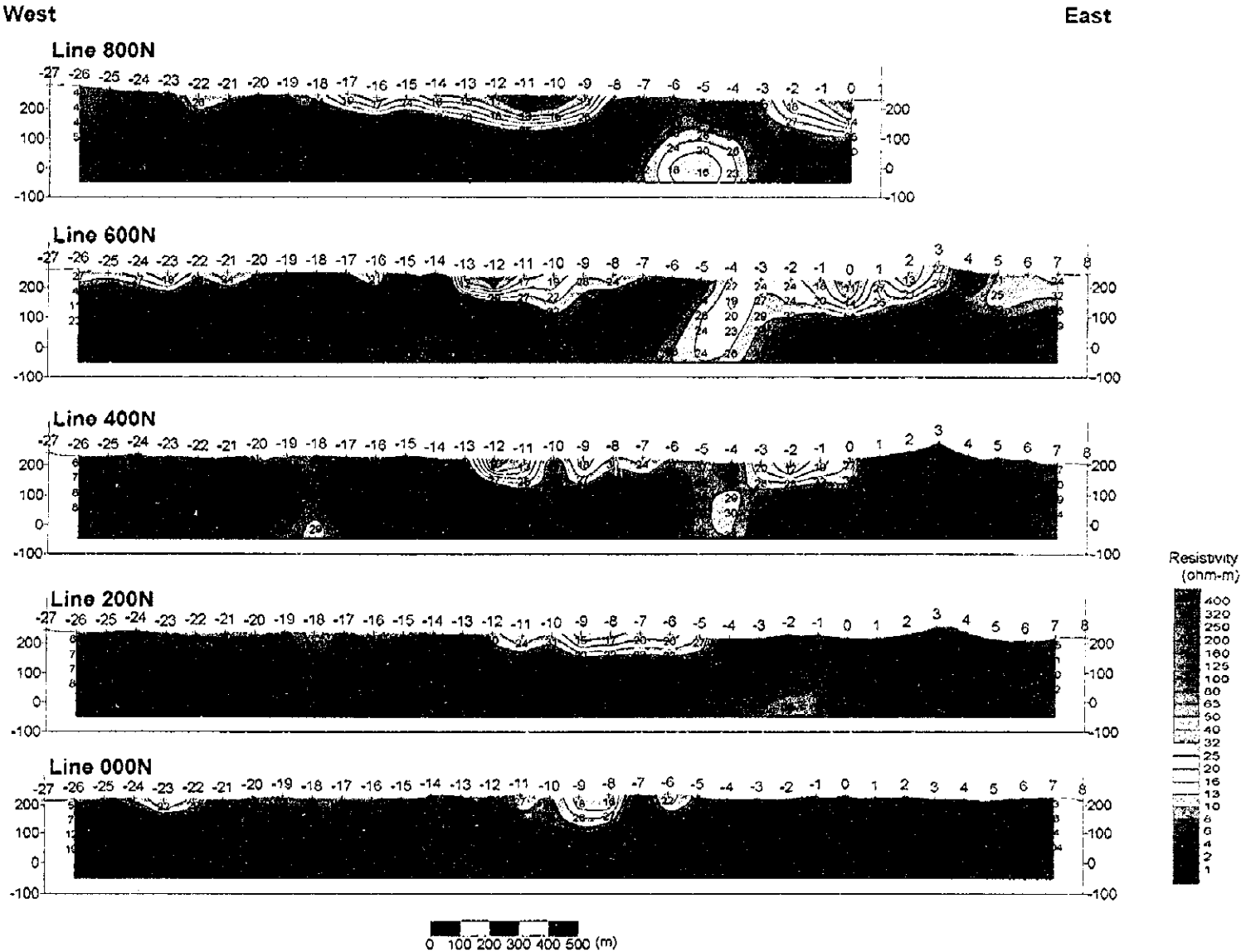

Fig. Ⅱ-2-26(1) IP resistivity model simulation on Doqal area

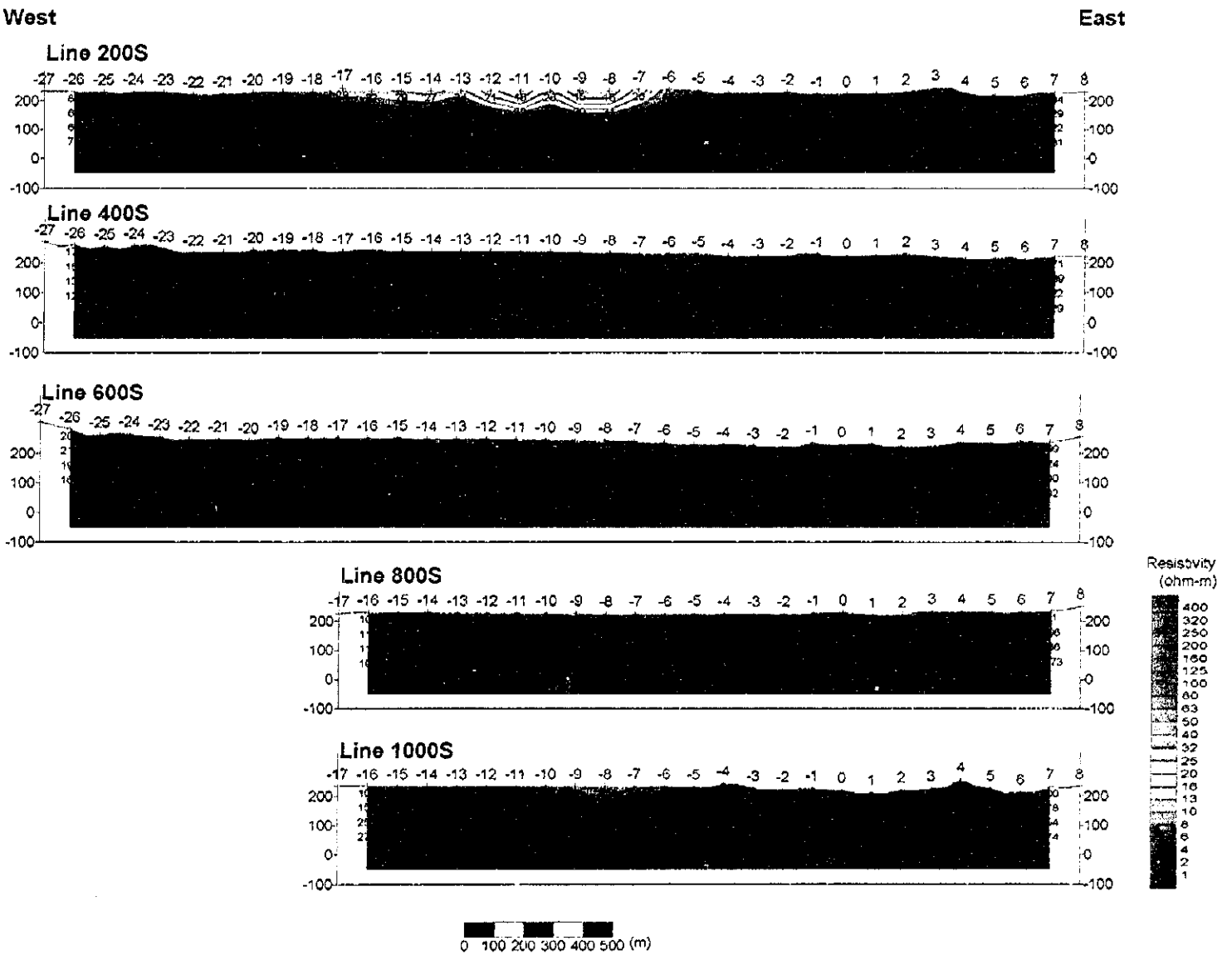

Fig. II -2-26(2) IP resistivity model simulation on Doqal area

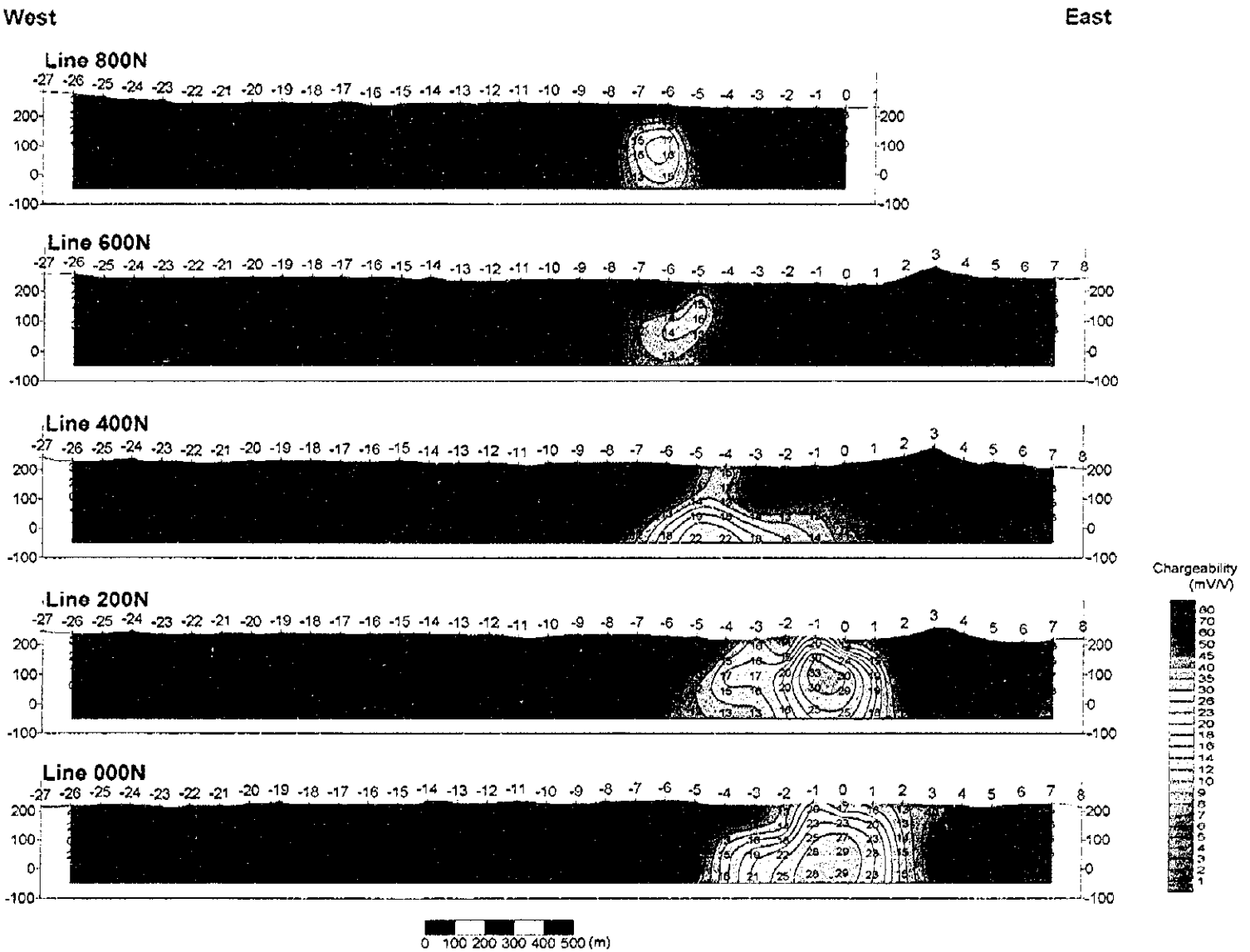

Fig. Ⅱ-2-27(1) IP Chargeability model simulation on Doqal area

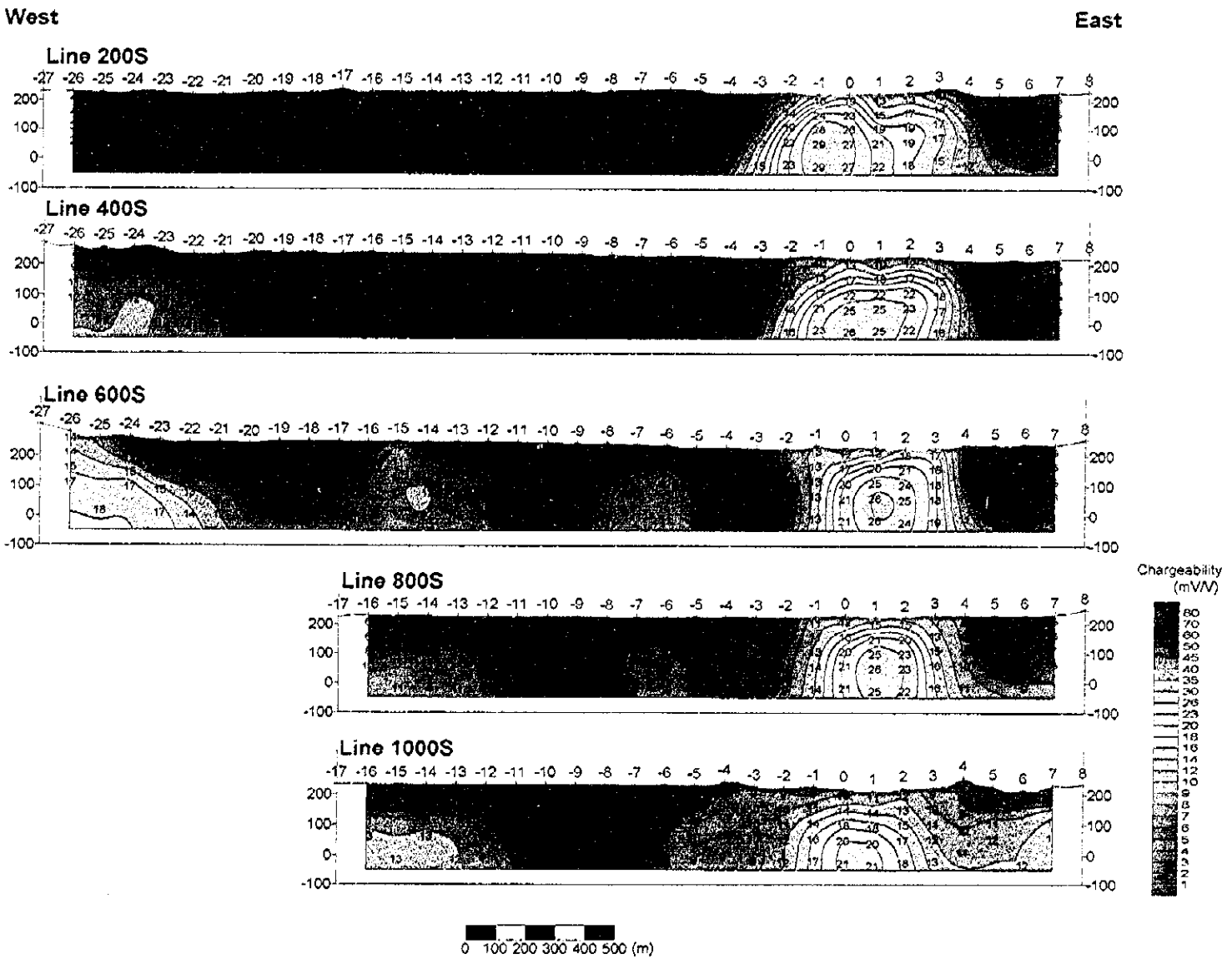

Fig. Ⅱ-2-27(2) IP Chargeability model simulation on Doqal area

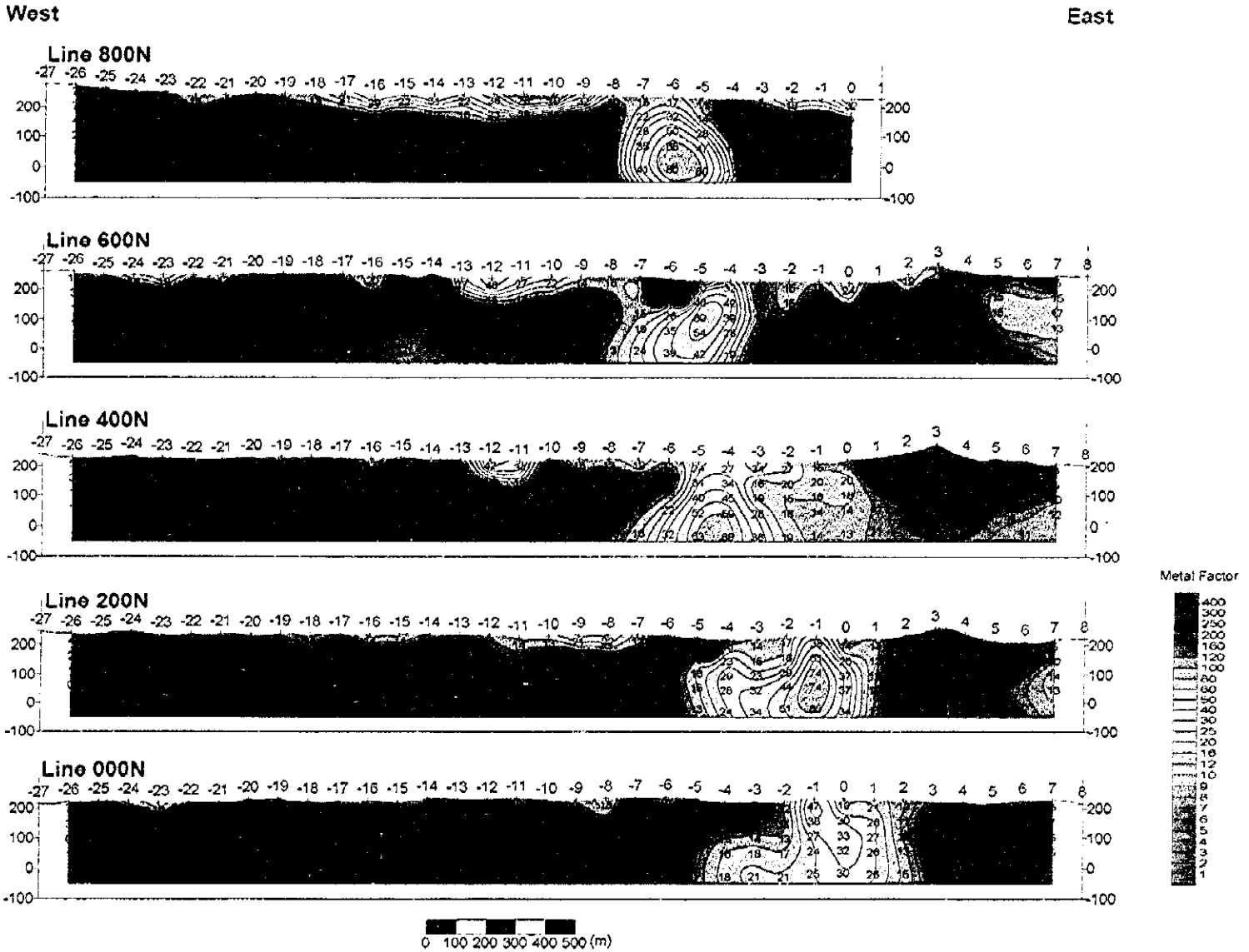

Fig. II-2-28(1) IP Metal factor model simulation on Doqal area

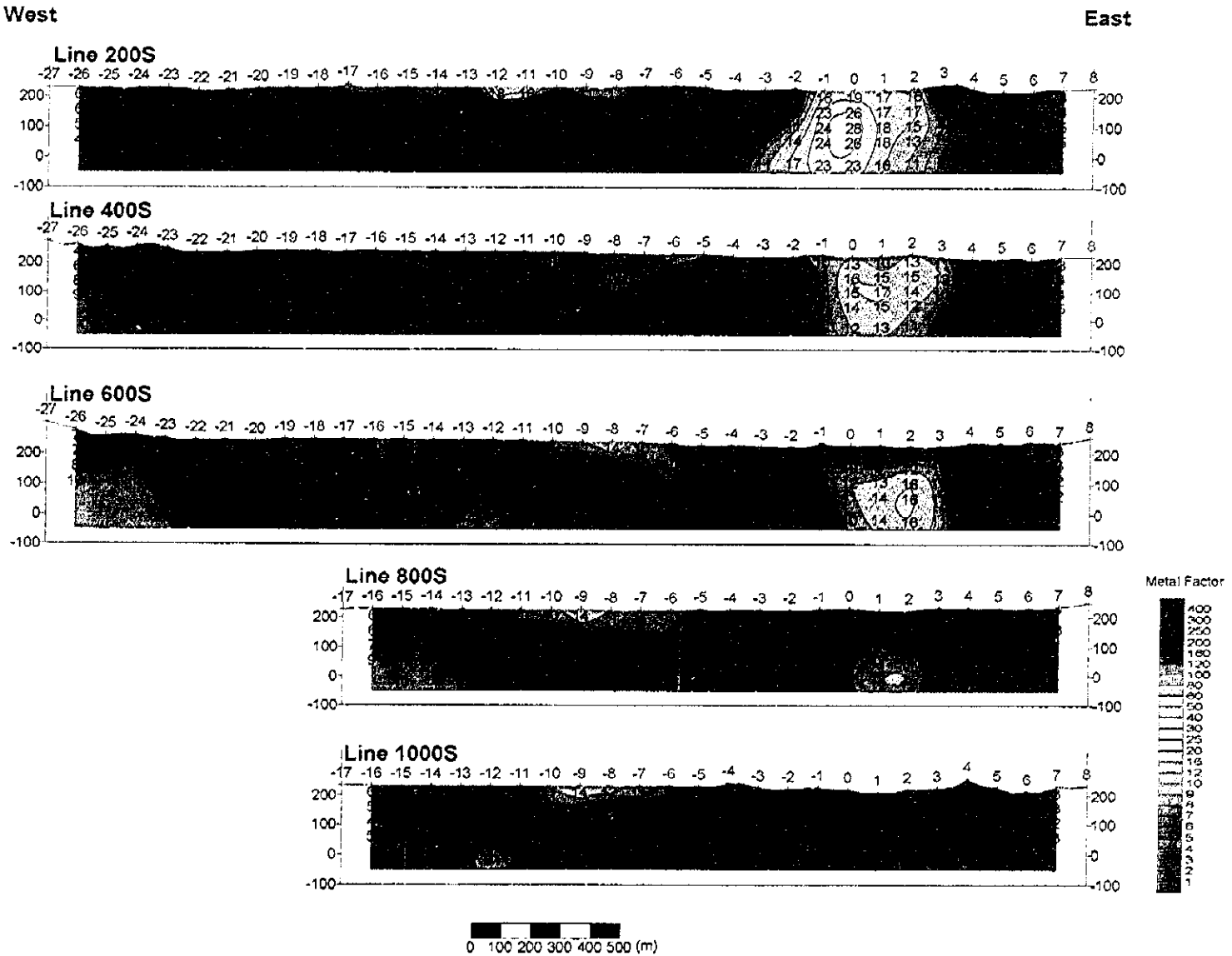

Fig. II -2-28(2) IP Metal factor model simulation on Doqal area

CHAPTER 3 TEM SURVEY

3-1 Background and Objectives

The TEM (Transient Electro-Magnetic) survey, sensitive to conductive bodies, such as massive sulphide deposits, was conducted to clarify the nature of the sulphide mineralization within the area delineated by the results of the TDIP survey.

Depending on the main objective, two different configurations were utilized during the 1997 field survey season, i.e., large fixed loops and small moving loops.

Taking into consideration the remarkable response given by conductive materials, such as massive sulfides, this detailed method is useful to extract promising mineralization zones by estimating their locations and boundaries. If drilling exploration confirms a massive sulphide body in the area under exploration, a program for small TEM loops is carried out in order to delimit its size, depth and extension.

3-2 Survey Locations and Specifications

Among the promising results obtained by the TDIP method, the geophysical TEM survey method by using large fixed loops were utilized in Daris, Doqal and Ghuzayn areas. From the good results obtained during the 1996 and 1997 field surveys, a program of small loops was carried out in areas where new deposits were discovered, i.e., in GArea1 (ore body No. 3), GArea2 and GArea3 (ore body No 1).

The amounts of survey carried out in the areas of Daris, Doqal and Ghuzayn by using the TEM geophysical method are presented in Table II-3-1 .

Table II-3-1 Survey amounts of TEM

CONFIGURATION	AREA	NUMBER OF LOOPS	NUMBER OF POINTS
LARGE	Daris	2	162
	Doqal	2	162
	Ghuzayn	2	153
	Sub-total	6	477
SMALL	Ghuzayn Garea1	19	19
	Ghuzayn Garea1	46	46
	Ghuzayn Garea2	39	39
	Ghuzayn Garea3		
	Sub-total	104	104
	TOTAL	110	581

3-3 TEM Survey Method

3-3-1 Basic Principles

The principle of the TEM system used in this survey is to energize an ungrounded loop situated on the surface of the earth, as illustrated in Fig. II-3-1. When the currents flowing in the loop are switched off, free electron conduction currents are induced (called eddy currents) in the ground. The eddy currents are known to depend on the conductivity, size and shape of the conductive body, and position with respect to the sensing loop. These eddy currents set up a secondary magnetic field which can be detected by a receiver coil as a time-dependant decaying voltage (See Fig. II-3-2).

The measurement of the time dependent decaying voltage is a means of detecting conductors in the ground. This transient decay can be measured by a number of measurement channels recording the voltage at various delay times after the transmitted fields are switched off.

According to Faraday's law, the quick shut-off of the primary magnetic field caused by the current termination, induces a pulse of emf (voltage) in the surrounding media. The resulting eddy currents produced in nearby conductive material support a surrounding secondary magnetic field for the duration of the pulse. Thereafter, with no external emf to support it, this system of currents and magnetic field decays with time, and it is this transient magnetic field which the receiver measures. These measurements occur during fixed time "windows" which occupy most of the "off-time" of the transmitter. Since the receiver must know when the transmitter is off, synchronization was done by using crystal clocks.

3-3-2 Logistics and Data Acquisition

There are several varieties of TEM systems and modes of operations. During this survey it was used two kinds of configurations: large fixed-loop and small in-loops. For the case of large loops, a large, single-turn square loop of wire of 600m by 600m is laid out on the ground. A portable power generator of 2500 W fed a transmitter, which provides a series of alternating bipolar currents pulses with slow exponential turn-on and a rapid linear turn-off precise current waveform through the loop. After the transmitter loop has been set up, a small portable multi-coil receiver is moved to stations inside the loop. the receiver apparatus is moved along surface lines. Lines were surveyed within the loop to a distance of 100m away from the loop and the grid interval between the observed points was 50m.

The small loop configuration uses a single-turn square loop of wire of 50m by 50m and the receiver is placed in the center of the loop.

Previous to the data gathering, the crystals of the transmitter and receiver are warmed up before

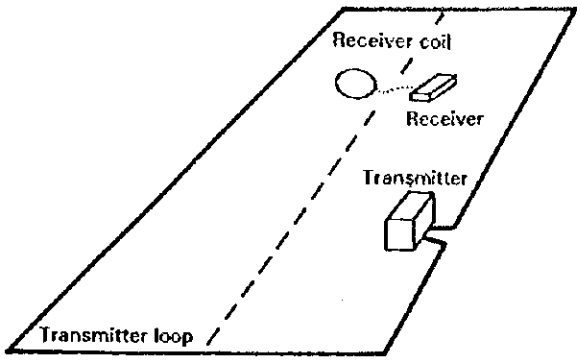

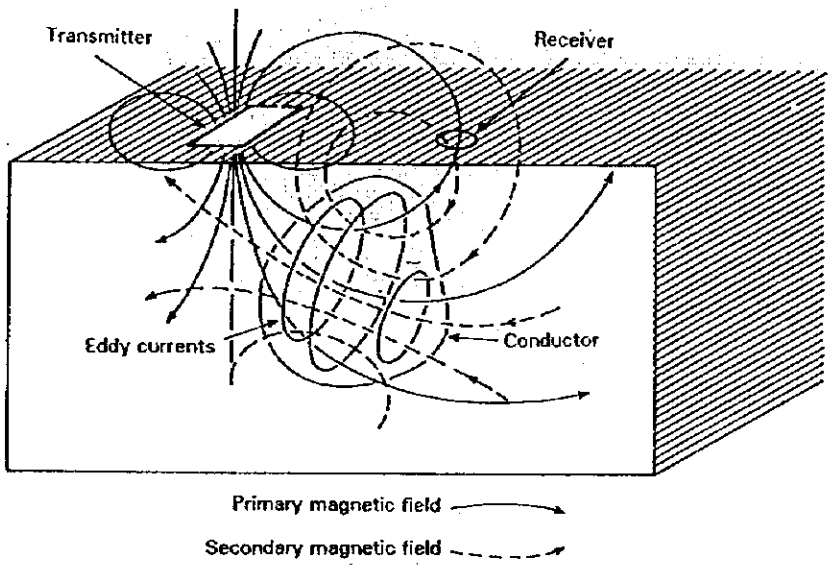

Fig.II-3-1 Schematic TEM survey configuration

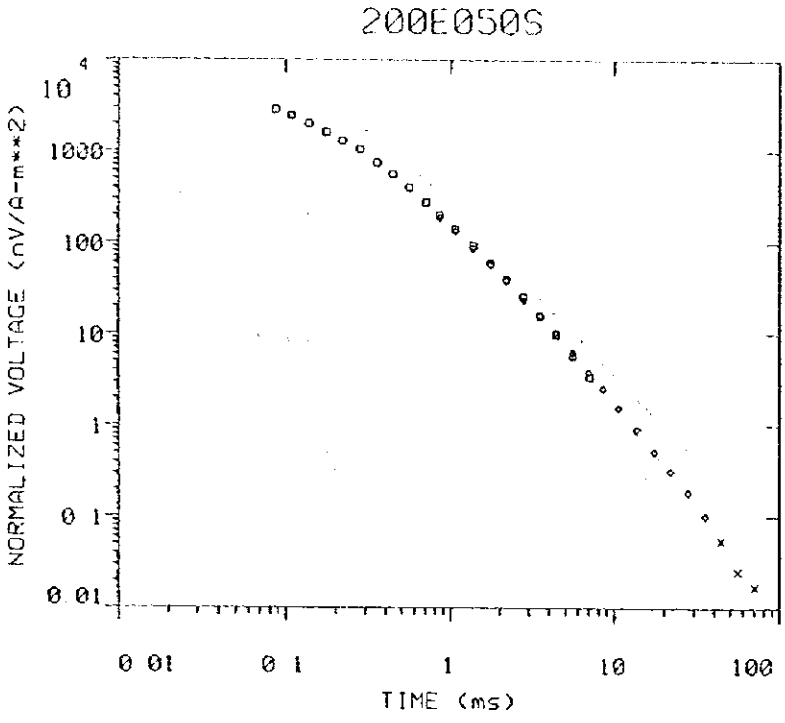

Fig.II-3-2 Example of TEM decay curve

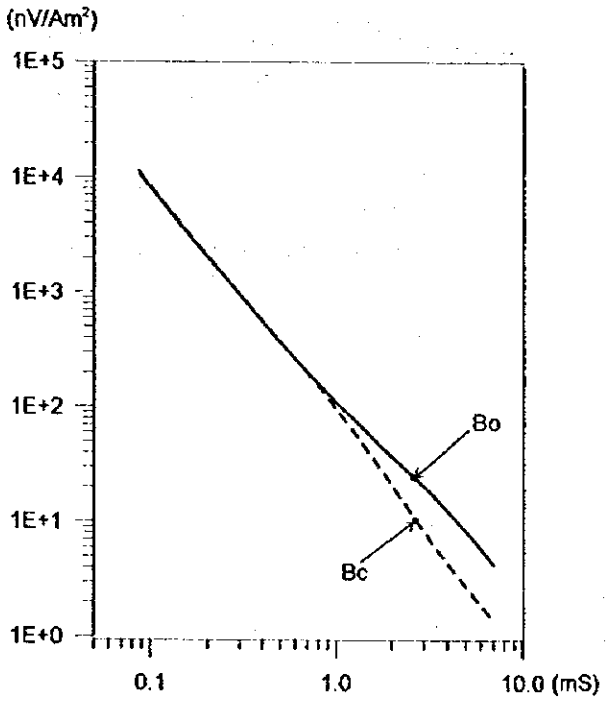

Fig. II -3-3 Observed and background TEM responses

attempting to synchronize. Synchronization of the transmitter and receiver was carried out using the built-in high stability quartz crystal oscillators. Integration for each measurement was carried out over 2^8 cycles.

The current waveform driven through the transmitter loop, and the number of spacing of channels in the receiver are the main distinguishing features of this method. 20 time channels with locations and width are shown in Table II-3-2. Successive operations at 25Hz, then 2.5Hz, effectively gives 30 channels covering range from 88 μ sec. to 72 msec. A steady current is terminated rapidly by a 220 μ sec ramp in large loops and 40 μ sec in small loops.

During data collection, several transient decays are recorded for each sounding. Readings are acquired at several receiver gains with opposite receiver polarities for each sounding location to eliminate any cultural noise. Many pulses of positive and negative polarities are stacked in a short period of time and averaged to remove any disturbance. Finally, the readings are stored in a DAS-54 data logger and transferred to a PC for processing.

Table II-3-2 Channel times after switch off

Channel No.	Sampling time	Window width
1	88 μ s	18 μ s
2	110	24
3	140	36
4	177	37
5	220	40
6	280	72
7	355	76
8	443	100
9	564	142
10	713	156
11	881	180
12	1096	250
13	1411	380
14	1795	390
15	2224	500
16	2850	720
17	3600	780
18	4490	1080
19	5700	1420
20	7190	1560

3-3-3 Equipment Specifications

The EM37 system is a ground transient EM system manufactured by Geonics Ltd. of Canada with the following specifications:

Table II-3-3 Specifications of TEM survey instruments

Items	Specifications
Transmitter	Max output, 30A, 180V
Generator	5HP, 120V, 3phase, 400Hz
Receiver	25Hz:0.088-7.19ms
	6.25Hz:0.35-28.7ms
	2.5Hz:0.88-71.9ms
Magnetic Sensor	Induction coil
	Effective area 100m^2
Recorder	Model DAS54, 500kb

(1) EM37 Transmitter

Although the size of the EM37 transmitting loop can be varied, during the 1997 field survey, two configurations were utilized: (1) a single loop wire (4.5mm^2 copper wire) of 600 X 600 m and a current amplitude of about 12 Amp, and (2) a single small loop wire (2.5 mm^2 copper wire) of 50m by 50m and a current amplitude of about 20 Amp.

The current waveform in the transmitter consists of alternating bipolar current pulses with a slow exponential turn-on and a rapid linear turn-off. The base frequency of operation can be set at 2.5, 6.25 or 25 Hz, with corresponding window times of 71.9, 28.7, or 7.17 ms respectively. In this survey we used a base frequency of 25 Hz Transmitter motor generator: 5 HP Honda gasoline engine coupled to 120 volt, 3 phase, 400Hz alternator.

(2) EM37 Receiver

ITEMS:	SPECIFICATIONS:
Measured quantity	Time rate of decay of magnetic flux
Coil Sensor	Air-cored coil of bandwith 40kHz
	100cm dia. By 7 X 5cm cross-section
Time Channels	20 with locations and width as Table II-3-2
Synchronization to Tx	Oven controlled quartz crystals
Receiver Battery	12 volt rechargeable Gel-cell

At the receiver the induced voltage in the coil is measured in millivolts. Using the effective area of the coil and the gain of the receiver, these measurements are converted to the time derivative of the magnetic field in nanovolts/amp-meter^2

3-4 Analysis Method

3-4-1 General Approach

The fact that the primary field is absent during measurement time, leads to "cleaner" data which is easier to interpret. The rate of decay of a conductor's magnetic field depends primarily on its size and conductance. Eddy currents decay rapidly in poor conductors, while those due to good conductors decay slowly, and the timing of the channels is such that only the effects of eddy currents due to the good conductors are seen in the later channels. In conductive environments, therefore, the response from overburden and uneconomic ore deposits should be minimal in the later channels where the target response predominates.

The first step in data processing is to average the emfs (voltages) that are recorded at opposite receiver polarities. Then, the records at different amplifier gains are combined to give a single composite transient decay. After the composite transient decay has been calculated for each measurement point, the late stage apparent resistivities are calculated by using the following equation:

$$\rho_a(t) = \frac{\mu^{5/3} M_r^{2/3}}{20^{2/3}\pi} \cdot \frac{M_t^{2/3}}{t^{5/3} V^{2/3}}$$

Where V is the voltage measured at the receiver, Mr is the moment of the receiver, Mt is the moment of the transmitter, μ is magnetic permeability, and t is the time measured after transmitter switch off.

The TEM response detected in the receiver, depends not only on the electrical properties of the ground, but also on the location of receiving points and transmitter loop size, generally the highest response are observed at the center of the loop. To correct the response due to the receiving location, the following procedure was carried out:

From the TEM data obtained at the center of the transmitter loop, a layered resistivity structure was calculated by using an inversion analysis which assumes that this electrical structure represents an average resistivity in the loop.

By using the parameters of this resistivity structure, a synthetic response Bc(x, y) was calculated at all the points within the loop by taking also into account the relative position between the receiver and transmitter loop. If the resistivity structure at a point is nearly same as the average resistivity structure, the observed EM response should be almost the same as the calculated synthetic response, resulting in a

minimal difference. On the contrary and if the average resistivity structure is not related to an anomaly but the point represents the location of the conductive body underlied, the response becomes extremely high as compared with the synthetic response, and therefore, the difference between the responses becomes high, i.e.,

$$B(x,y) = \log (Bo(x,y) / Bc(x,y))$$

where: B(x,y) is the difference of response, Bo(x,y) is the observed response, Bc(x,y) is the synthetic response, and log is the logarithm of base 10.

Contour map of the difference in the TEM responses permit the clarification of anomalies (if any) by the contrast in the TEM response values.

For the depth estimation, the following formula is used:

$$d = \sqrt{500 \rho t}$$

Where ρ is the average resistivity(Ωm), t is the time(msec) and d is the depth(meter)

3-4-2 Small Loops Approach

Fig. II-3-4 shows an example of a comparison between TEM responses of the two different configurations used during the 1997 field survey, i.e., between the large fixed loop of 600m by 600m and the small loop of 50m by 50m. The example shows two cases: (1) TEM results obtained in the site where the borehole G30 intersected massive sulphide, and (2) TEM responses obtained on the station 1650W700N located outside of the assumed boundaries of the orebody No. 3. By comparing both results, it is clearly seen that the deviation experienced from the small loop is more remarkable than the deviation generated from the large loop.

A quantitative analysis can be carried out by investigating the decay voltage (time derivative of the secondary magnetic field) for every channel. From these results, the resistivity structure formed by 15 layers are calculated by using multi-layered analysis techniques based on Occam's method to obtain a smooth model. The right side of Fig. II-3-5 shows the depth results based on the multi-layer analysis obtained from the smooth inversion techniques. The left side of same figure shows the apparent resistivity curve calculated from the model (synthetic curve) and the observed data.

A compilation of all the inverted soundings of every station serves as a guide to build a 2-D resistivity section for every line.

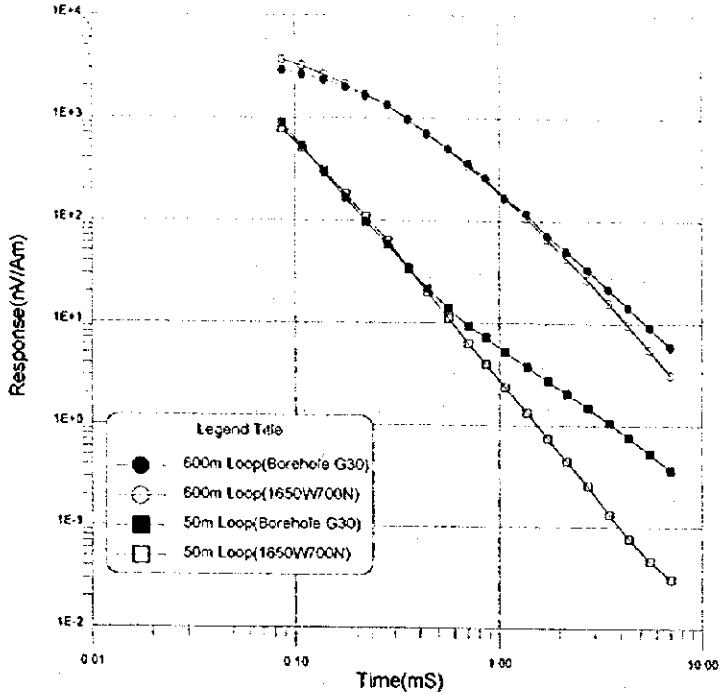

Fig. II -3-4 TEM decay response comparison between 600m and 50m loops

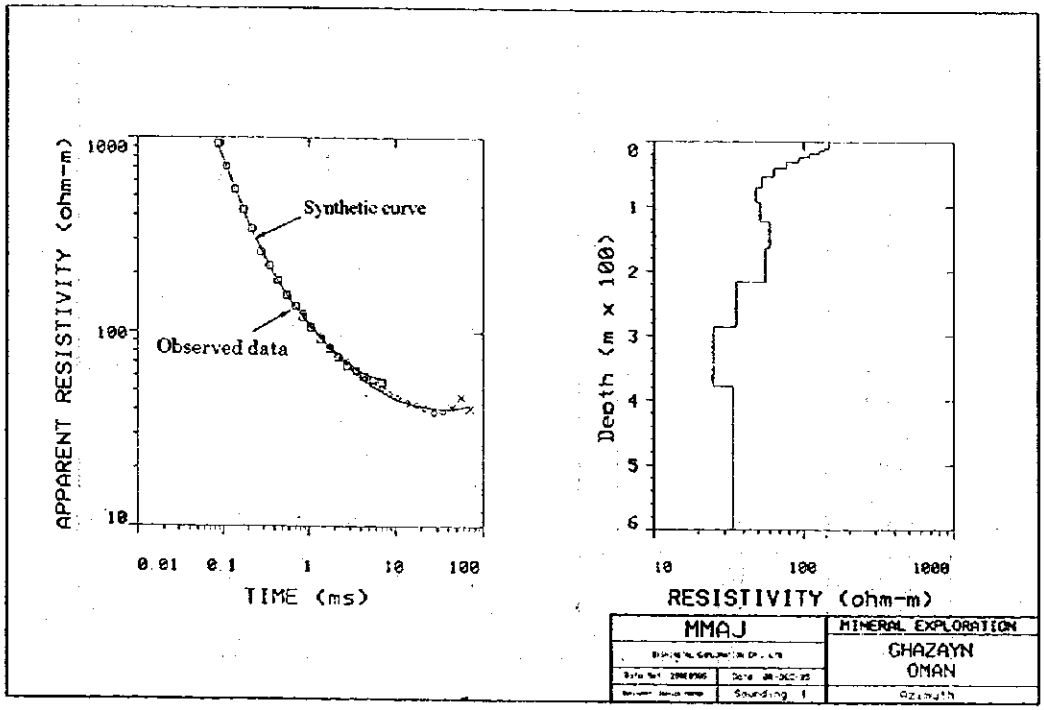

Fig. II -3-5 Multilayered resistivity analysis by Occam inversion method

3-5 Survey Results

3-5-1 Ghuzayn Area

(1) Loop Locations

As it was mentioned in Chapter 3, the TDIP survey of the lines 1200W to 2000W detected a remarkable anomaly along the line 1800W. To seek a more detailed study of this anomaly and its extension, a TEM survey was carried out around the anomaly. This study consisted of 2 large loops of 600m by 600m each and small in-loops of 50m by 50m on the newly discovered (ore body No.3) and its surroundings in order to provide appropriate locations for further drilling. Fig. II-2-4 illustrates the locations of the large loops as well as the small loops.

The estimated depth of investigation of the anomaly sources have been calculated taking into account the formula for exploration depth described in Section 3-4 of this Chapter. Table II-3-4 shows the estimated depth in the 2 large loops surveyed in Ghuzayn area as a function of the channel times. Since these values are calculated for a layered resistivity structure at the center of the loop, the calculated depth should be taken with caution because it does not always correspond to the real depth.

Table II-3-4 Depth estimation in survey area

Unit: meter

	Ghuzayn		Doqal		Daris	
Channel	Loop1	Loop2	Loop1	Loop2	Loop1	Loop2
Ch1	25	39	39	38	45	41
Ch2	28	44	44	43	50	46
Ch3	32	49	49	48	56	52
Ch4	36	55	56	54	63	58
Ch5	40	62	62	61	71	65
Ch6	45	69	70	68	80	73
Ch7	51	78	79	77	90	83
Ch8	57	87	88	86	100	92
Ch9	64	99	99	97	113	104
Ch10	72	111	112	109	127	117
Ch11	80	123	124	121	141	130
Ch12	89	137	138	135	158	145
Ch13	101	156	157	153	179	165
Ch14	114	176	177	173	202	186
Ch15	127	196	197	192	225	207
Ch16	144	222	223	218	254	234
Ch17	162	249	251	245	286	263
Ch18	180	278	280	273	319	294
Ch19	203	314	316	308	360	331
Ch20	228	352	355	346	404	372

(2) Results

(a) Large Loops

Loop 1

A map showing the results of the TEM response in the Loop 1 is presented in Figs. II-3-6(1) and (2). Two remarkable TEM anomalies are seen, one in the central part of the loop and another one, in two places around the NE part of this loop.

The first anomaly can be clearly seen by an abrupt change in channel 16 of a high anomaly in the form of an oval shape along NS direction and assumed to be extended outside of this loop. Estimated size of this oval shaped anomaly is about 250m in the east-west direction and more than 250m along the north-south direction. Along the main axis of this anomaly the boreholes G30, G31, G32 and G33 were sited. As a results of these drillings, a massive sulphide deposit was intersected at a depth of about 100m and specially the boreholes G30 and G31 intersected the deposit with a thickness between 70 and 90m and getting thin northwards.

In relation to the second anomaly, from the channels 1 to 12 it is seen an anomaly trending north-east at a shallow depth. Due to the low chargeability values detected at this level, it is presumed that this anomaly does not bear any relation with mineralization but rather caused by a shallow conductor, such as saline underground water, weathered layer.

Loop 2

TEM results are indicated in the Figs. II-3-7(1) and (2).

A high TEM response is seen towards the central part of the loop along the north direction and centered around the station 1400W600N. Since this anomaly is clearly detected in the channels 6 to 12, it is assumed to be distributed at shallow depth. Also the response is not strong enough to be considered due to a massive sulphide conductor, but rather related to high salinity of the underground water or a weathered layer.

(b) Small Loops

Based on the discovery of the ore body No.3 and the TEM results of the large loops carried during the 1996 field survey, a program of small 50m by 50m in-loops was carried out in small areas within Ghuzayn, i.e., GArea1, GArea2 and GArea3.

Fig.II-2-4 shows the locations of the small loops.

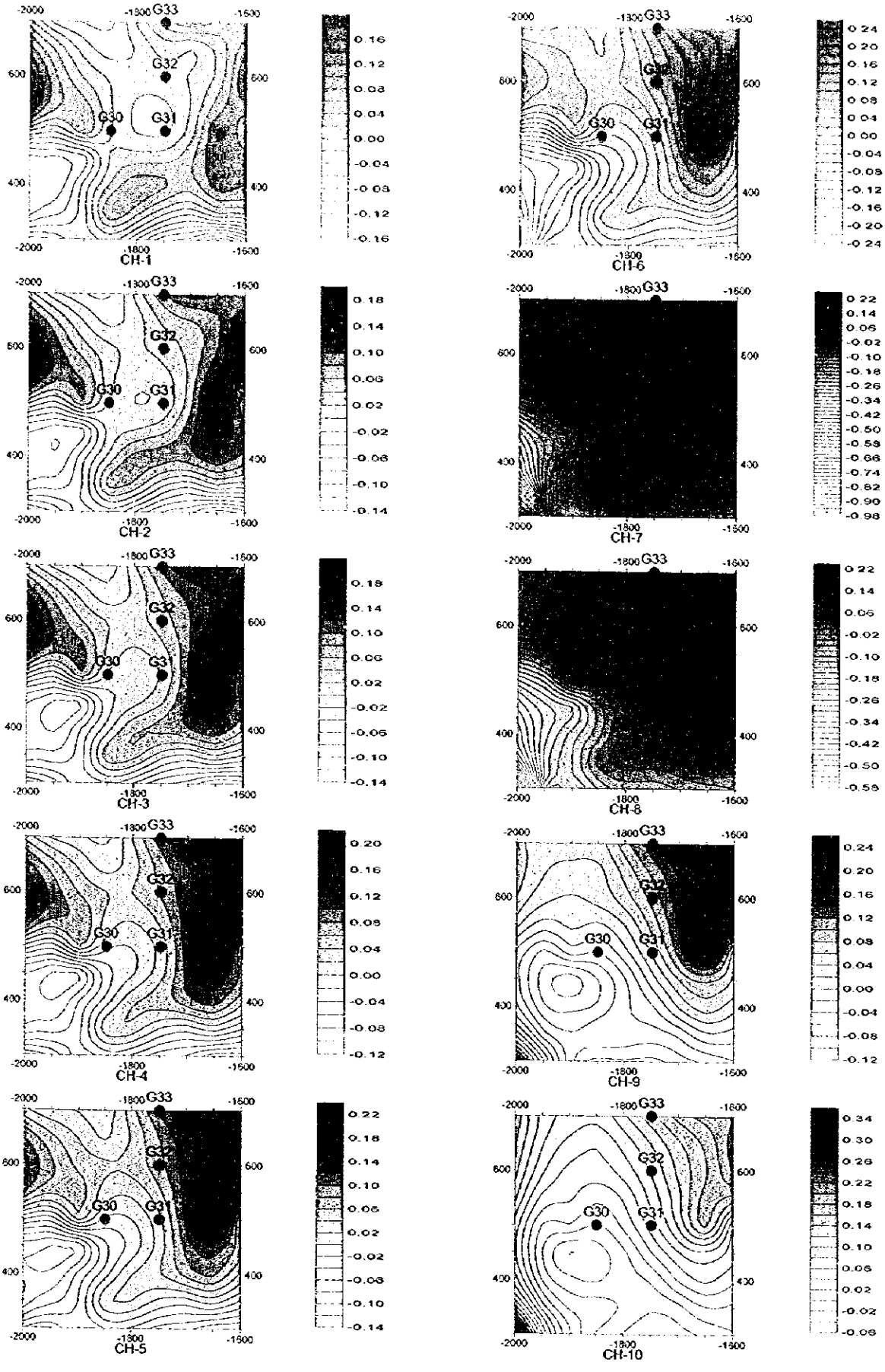

Fig. Ⅱ-3-6(1) TEM response maps of Loop1 in Ghuzayn area(Ch1-Ch10)

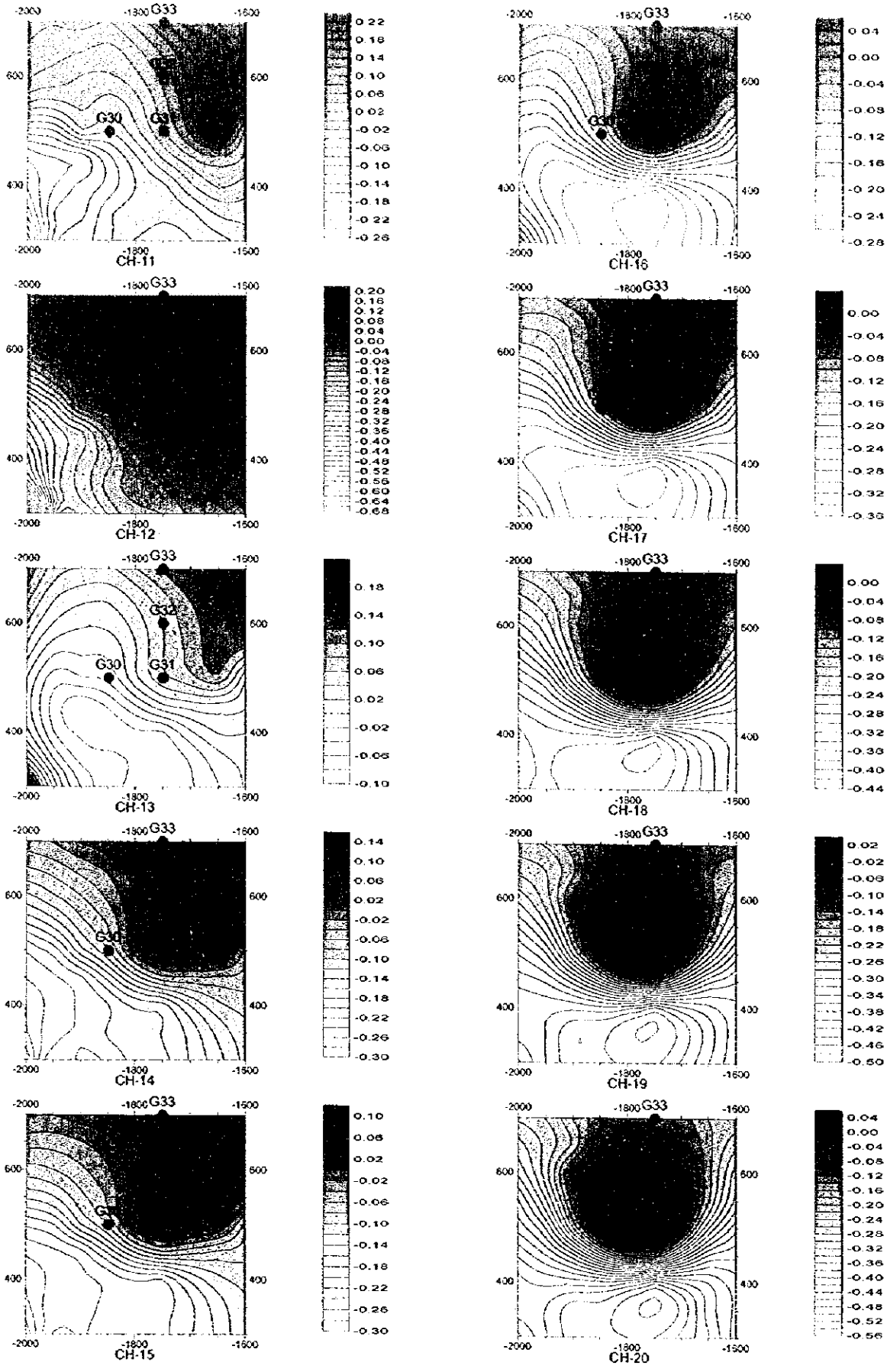

Fig. II -3-6(2) TEM response maps of Loop1 in Ghuzayn area(Ch11-Ch20)

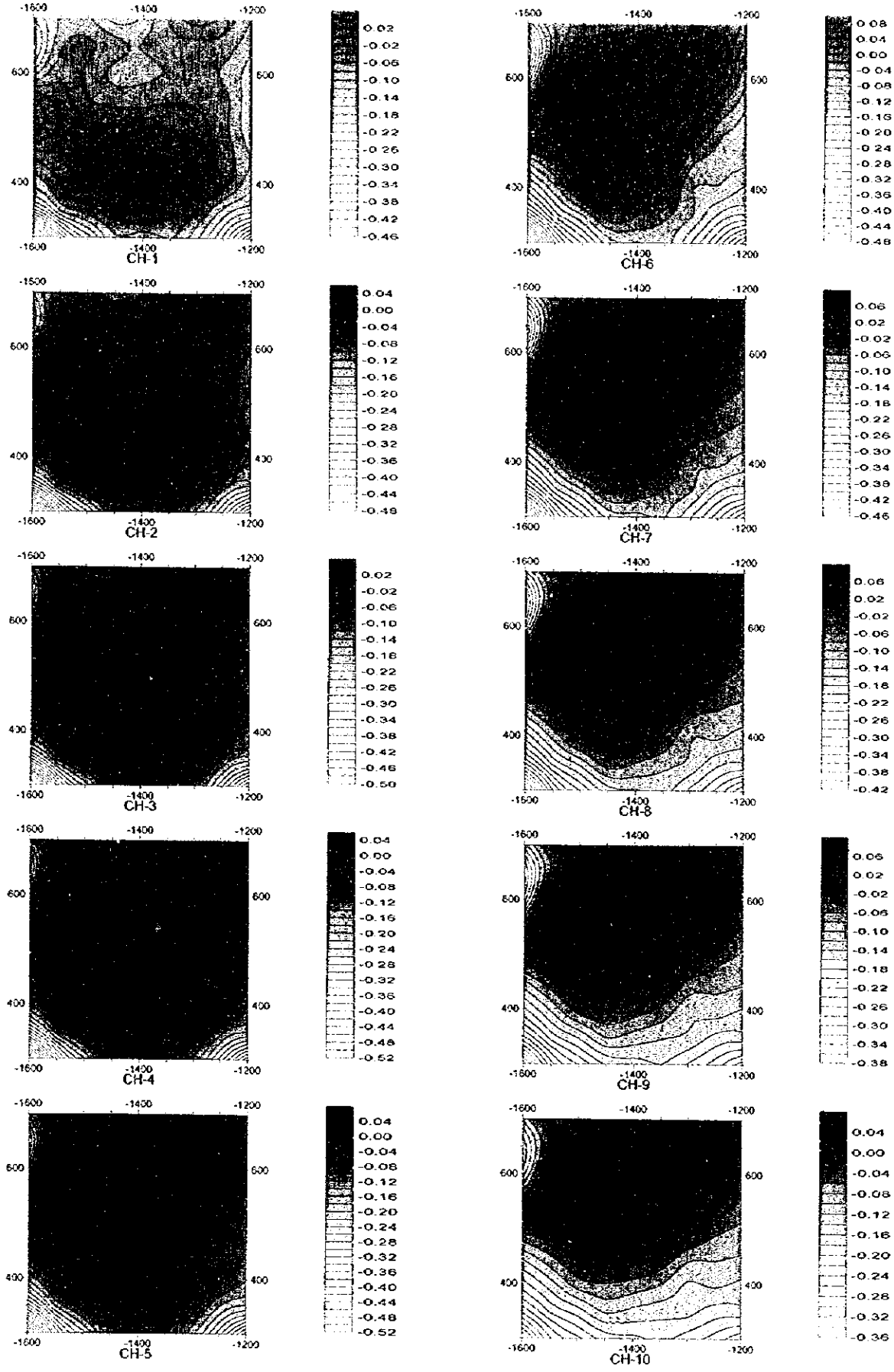

Fig. II-3-7(1) TEM response maps of Loop2 in Ghuzayn area(Ch1-Ch10)

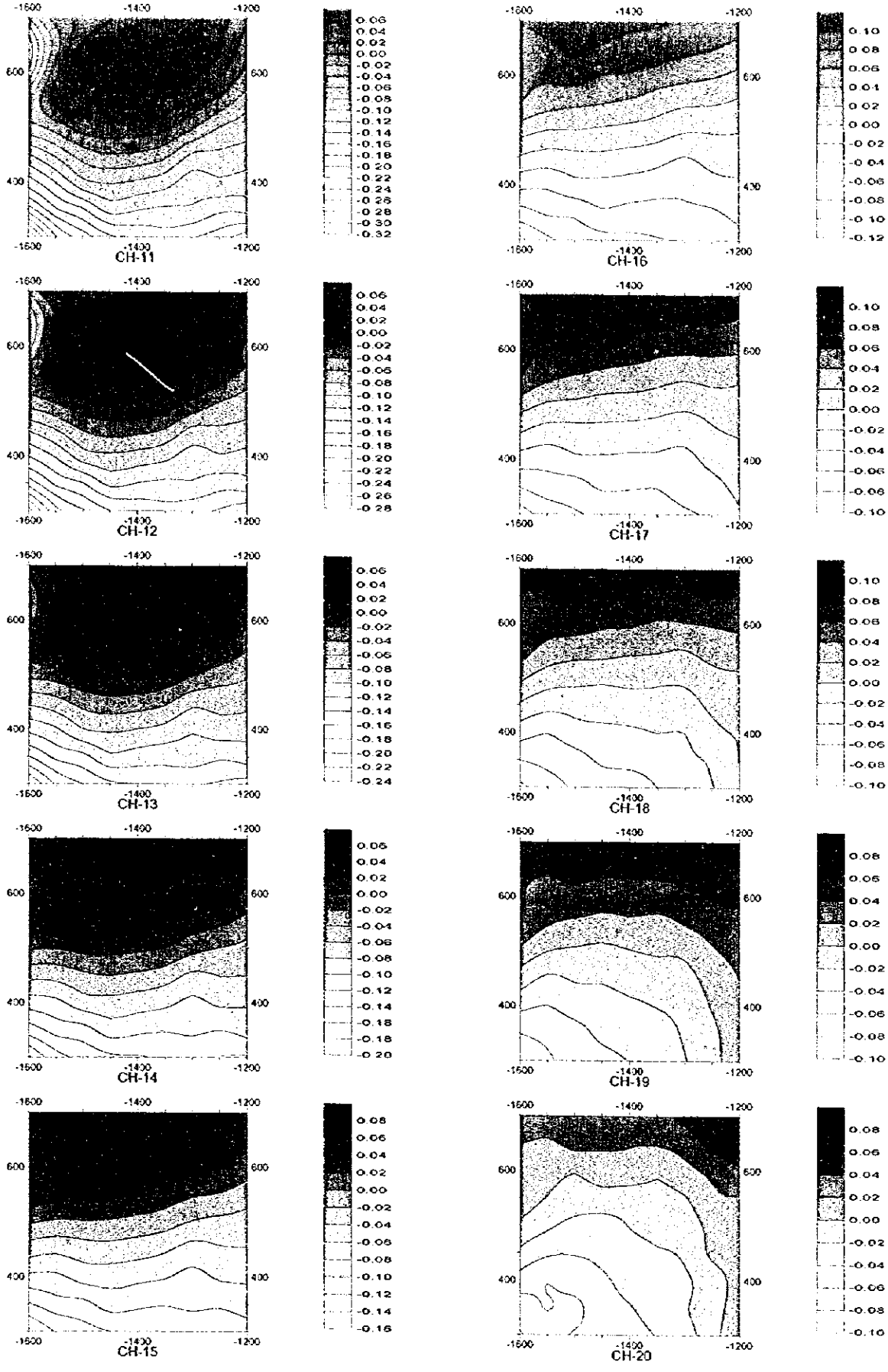

Fig. II-3-7(2) TEM response maps of Loop2 in Ghuzayn area(Ch11-Ch20)

GAreal

Fig. II-3-8 represents the TEM transient decay curves. In these curves, the vertical axis represents the time rate-of-change of the secondary magnetic field in units of 10^{-9} Volt/Amp meter^2, while the horizontal axis represents the sampling time in units of msec after the transmitter current is cut. It should be noted here that early times correspond to shallow layers and increasing time corresponds to increasing depth.

As indicated in the above mentioned figure, a total of 39 soundings (small loops) were acquired over the area of interest. In some cases during data acquisition, the rig and the vibration of the drilling machine had some negative effect on the data that they had to be omitted for the interpretation.

Other factors considered during interpretation of the transient decay curves seen in the figure, is that within 1 msec after the transmitter current is off, the attenuation rate of the TEM response in the early-time zone is relatively large (i.e., the slope of the curve is large), but after that, the decay rate becomes small because of a bigger secondary voltage coming from the ore body. This slow decay is the cause of the big TEM response seen in the curves. If the orebody is located at shallow depth, the decay rate appears small from early times and furthermore, the thicker the orebody, the longer is the duration of this slow decay.

During data interpretation, few of the soundings located to the west and north-west of the borehole G30 presented inconsistent data which is believed to be due to cultural noises along the north-south direction coming from a surrounding area where a power line is seen.

According to the above explanation and the results seen in Fig. II-3-8, the transient decay curves indicated in blue color show a slow decay-rate after 1 msec. On these grounds, it is a strong possibility that massive sulphide can be found below the station where these soundings were located. Taking into consideration these curves, it can be inferred that the massive sulphide deposit (orebody No.3) can be found extended about 400m along the north-south direction and about 250m along east-west direction.

As shown in Fig. II-3-9, further interpretation was carried out by constructing analyzed resistivity sections along selected profiles, i.e., line 1800W along north-south direction and the lines 500N, 600N and 700N along east-west direction. The profiles in this figure show also the boreholes and the location of the orebody as inferred by the boreholes. By comparing the borehole results and the analyzed resistivity results from the TEM survey, it can be said that the analyzed resistivity value of about 2 Ωm for the massive sulphide zone, matches well with the value of 1.5 Ωm obtained from electrical properties of the core samples analyzed in the laboratory.

On the above basis, a zone of less than 2 Ωm is observed along the line 1800N. This zone which is clearly seen around the station 500N at the shallow depth of about 100m, changes abruptly towards the south and deepens roughly 30° southward.

In the profile 600N it is seen that the zone of less than 2 Ωm deep down abruptly to the west of the

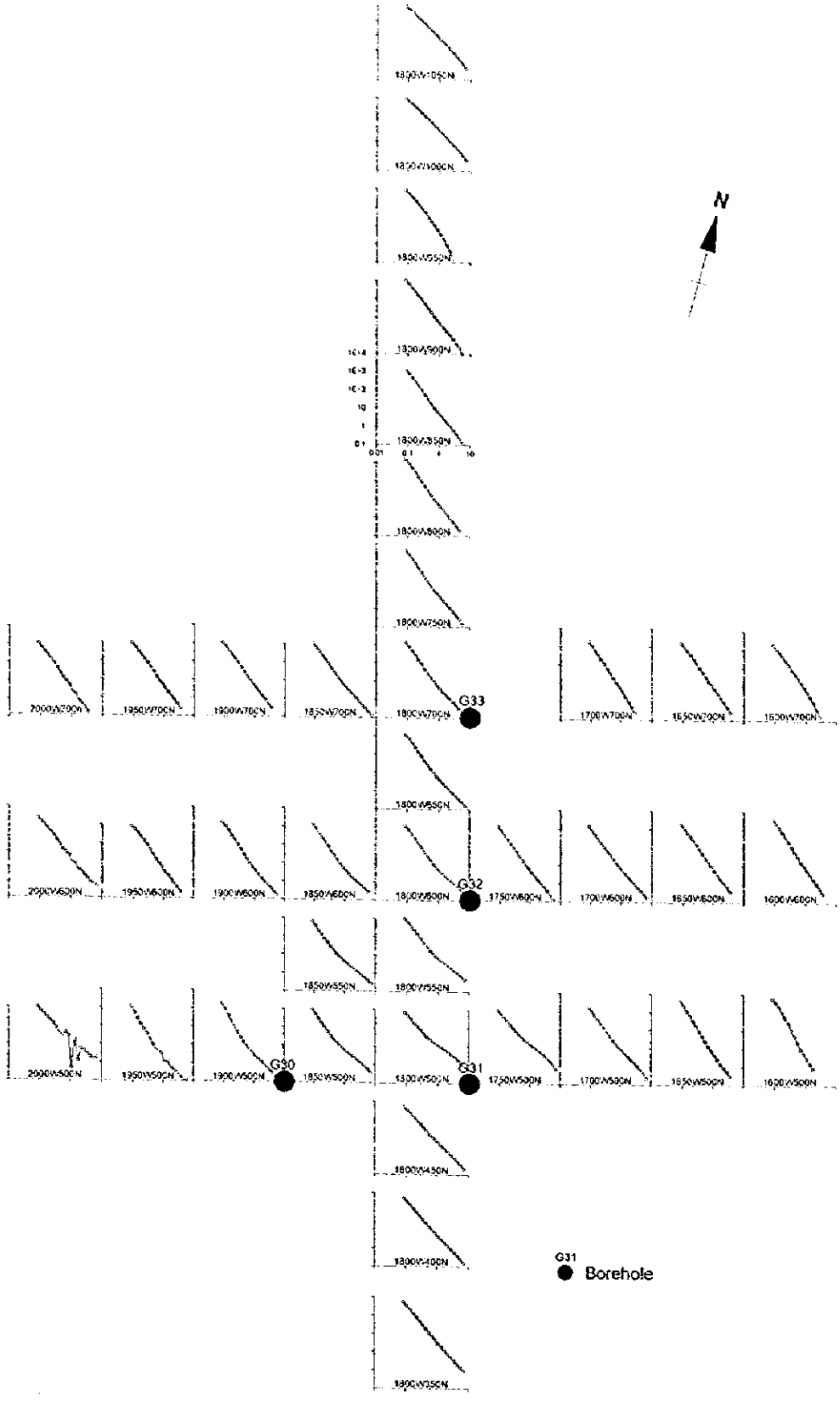

Fig. II -3-8 TEM response decay curves in Gareal of Ghuzayn area

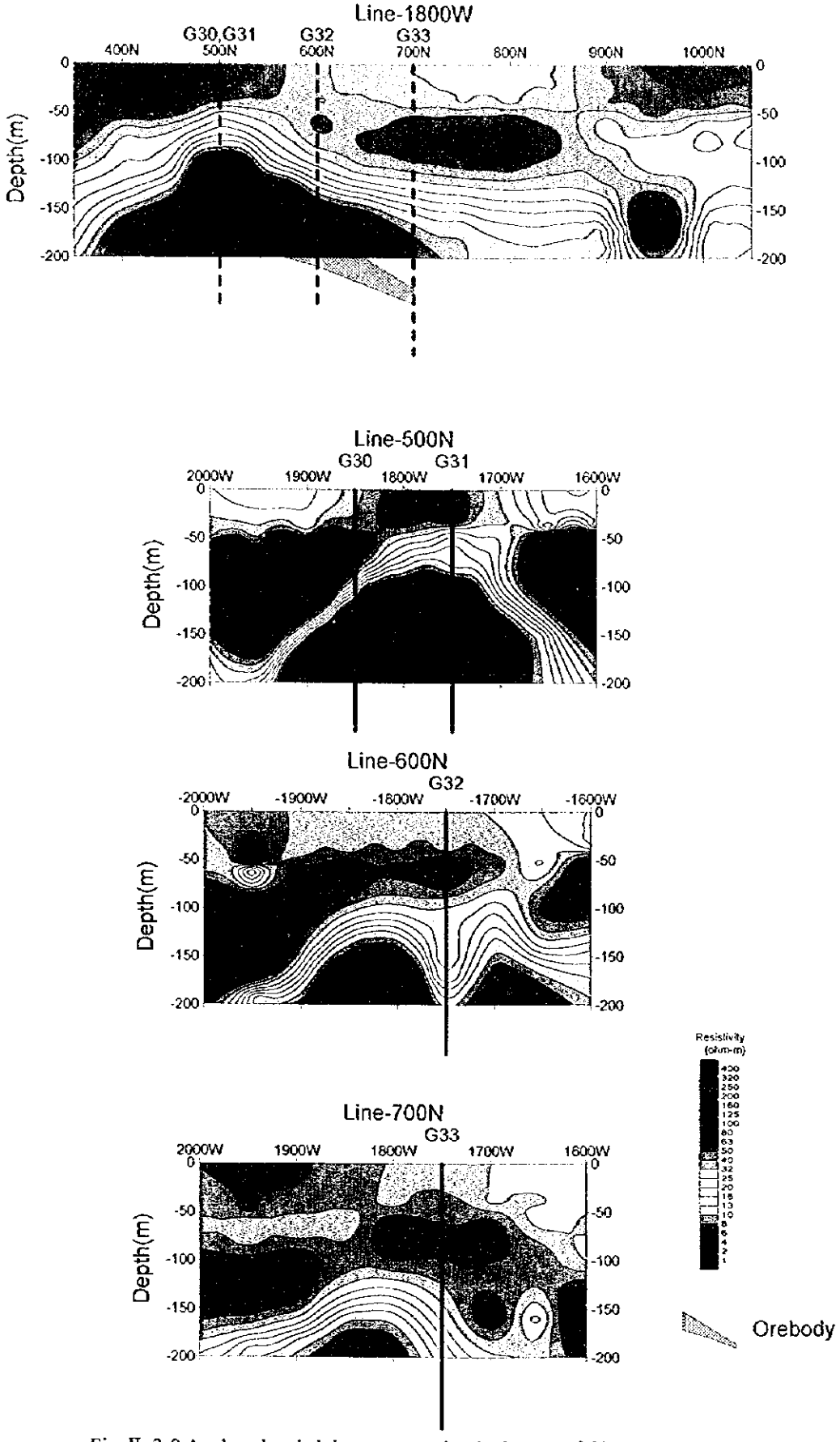

Fig. II -3-9 Analyzed resistivity cross-section in Gareal of Ghuzayn area

bore G30 and to the east of G31. In relation to the lines 600N and 700N, it can be inferred that towards the north the orebody is expected to be intersected at deeper levels. The low resistivity zone seen at a depth of 170m in the analyzed resistivity section 600N though not clear, is consistent with the results obtained in the borehole G32

GArea2

During the field season survey of 1996, a program for TEM large loops was carried out around the orebody 2. To further clarify the anomalies detected by the large loops, a program of small loops of 50m by 50m in size and consisting of 19 soundings was carried in the north-east part of the mentioned orebody.

Fig. II-3-10 shows the location of the soundings including the transient decay curves obtained in every station. Based on the slow decay rate seen in the early-time (within about 0.5 msec) TEM decay response of the curves around the borehole G23, it can be inferred the existence of a conductor body in the shallow part. After 0.5msec, the transient decay rate becomes bigger in most of the cases.

As a further interpretation, the Fig. II-3-11 indicates the analyzed resistivity structure obtained by using a multi-layer analysis along the line 75N which crosses the boreholes G23 and G24 along the east-west direction. To construct the profile, sounding data from the 6 stations from 625W075N to 325W075N were utilized. From this analysis, it can be inferred a low resistivity layer of about 10Ωm distributed almost from the surface down to several ten meters. A high resistivity zone of more than 100Ωm is seen distributed at deeper levels, but it becomes lower at much deeper levels.

GArea3

The boreholes G3 and G13 are located in this area where the orebody No.1 was discovered.

A TEM program consisting of 47 small in-loops were carried in order to investigate the possible extension of this deposit and satellite deposits.

Based on the results obtained from this survey, the boreholes G25 and G27 were drilled, however, only G25 intersected massive sulphide with a thickness of about 7.5m at a depth of 115m.

The Fig II-3-12 shows the location of the small loops carried in this area including the plotting of the transient decay curves on every station.

The transient decay curves observed in the stations between the boreholes G3 and G9 indicate after 1 msec a somewhat slow decay rate meaning that massive sulphide may be found hidden within this interval. However, since no remarkable TEM anomaly was detected in the surroundings of the orebody No.1 and since the range of the anomaly is rather narrow, it can be inferred that if massive sulphide is found it should be small in scale.

The Fig. II-3-13 indicates the results of a multi-layer analysis made along the lines 75W and 125S.

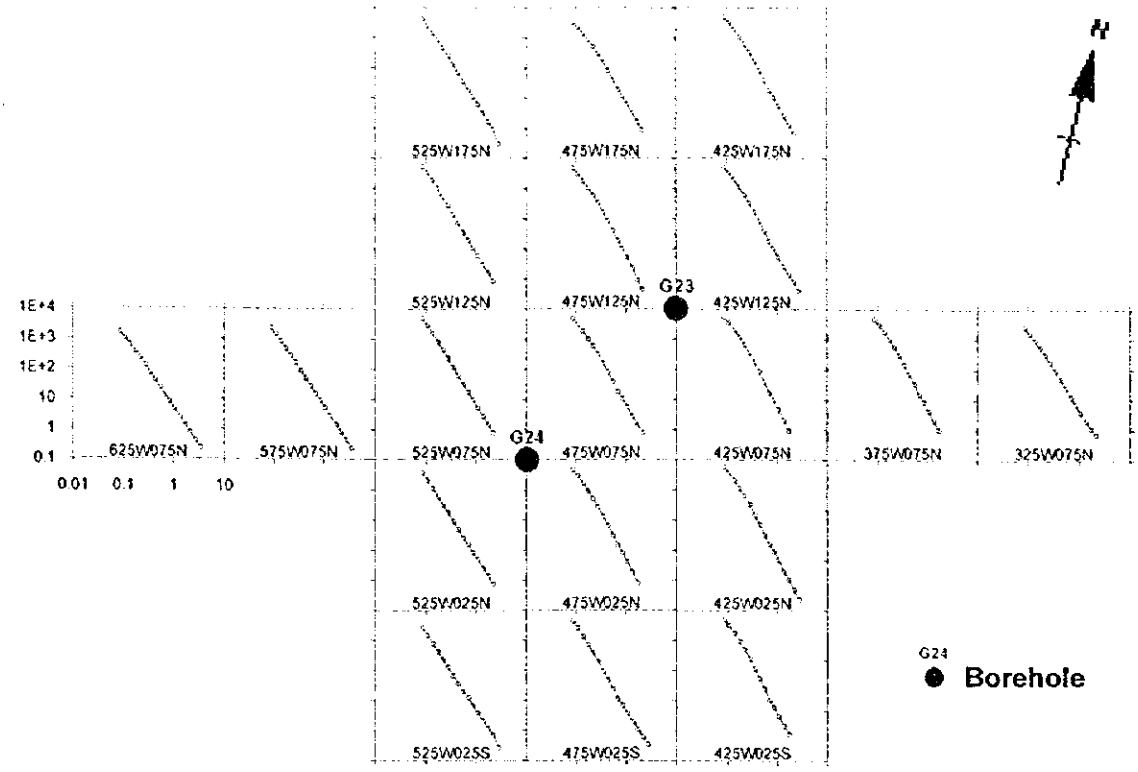

Fig. II -3-10 TEM response decay curves in Garea2 of Ghuzayn area

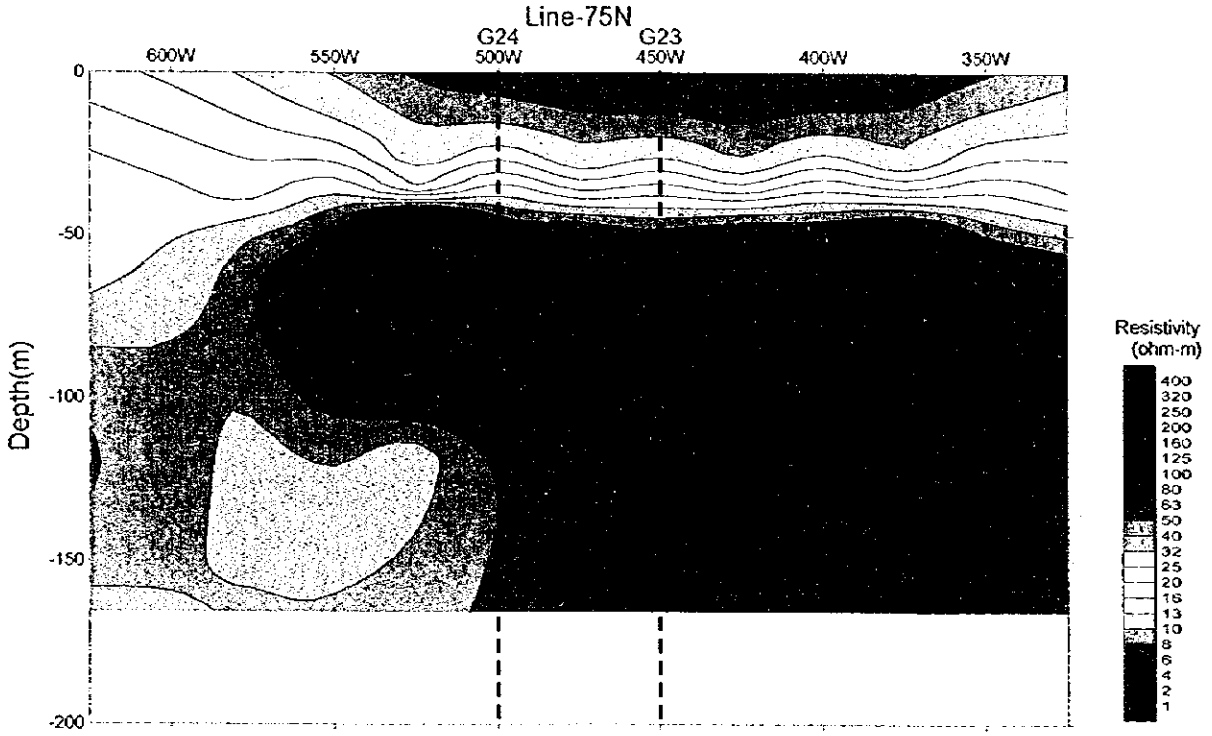

Fig. II -3-11 Analyzed resistivity cross-section in Garea2 of Ghuzayn area

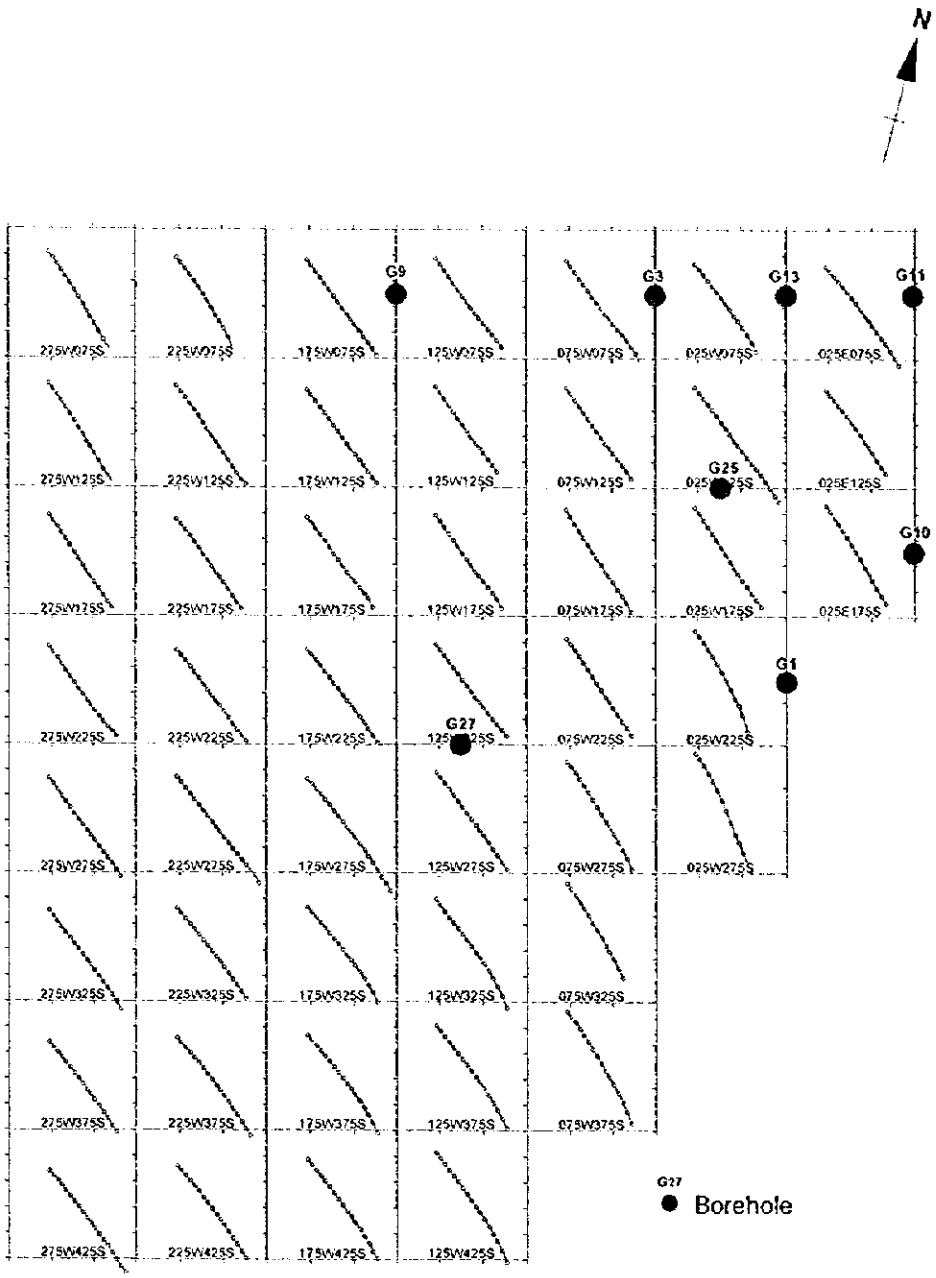

Fig. II -3-12 TEM response decay curves in Garea3 in Ghuzayn area

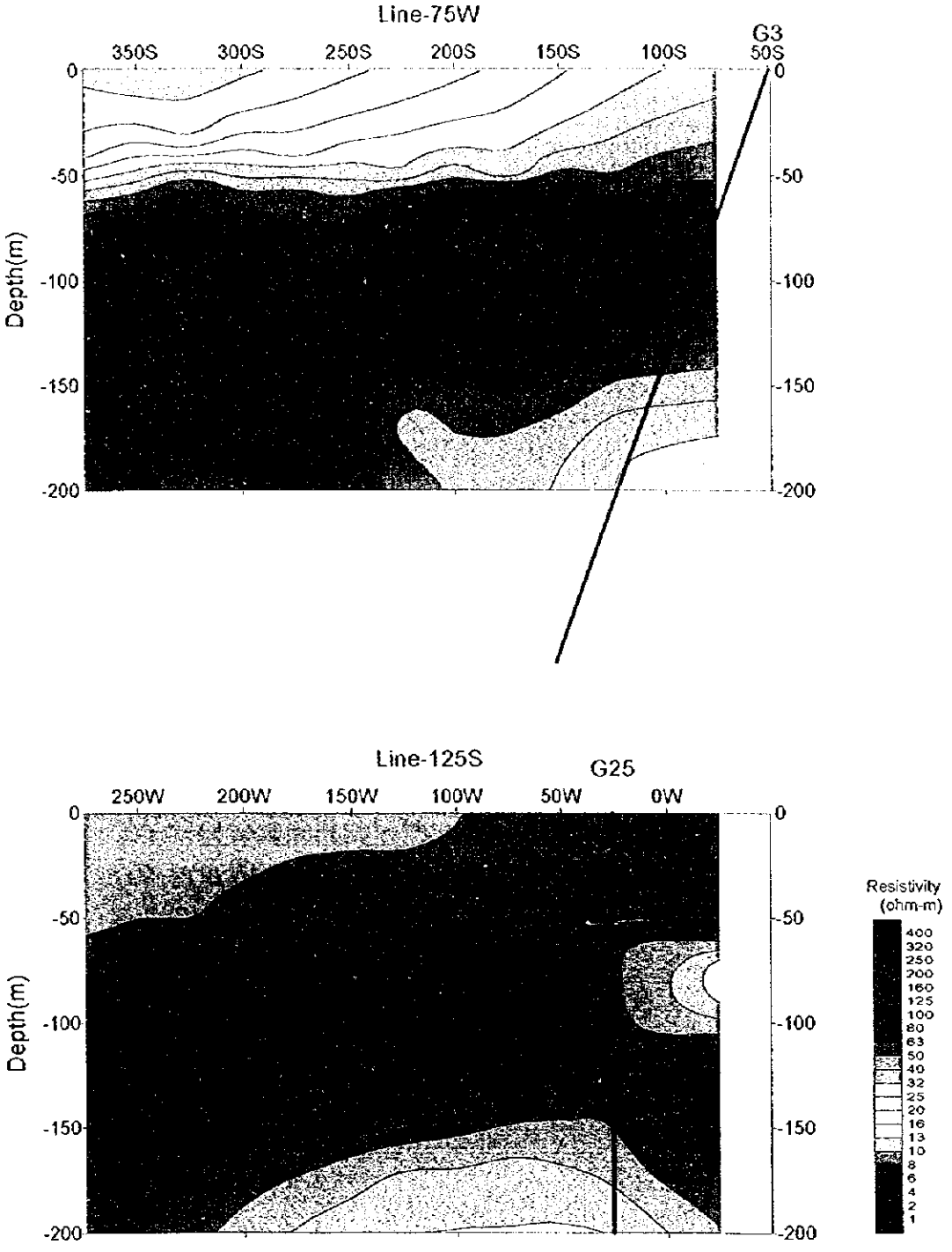

Fig. II-3-13 Analyzed resistivity cross-section in Garea3 in Ghuzayn area

According to these results, the line 75W shows a low resistivity distribution zone between the stations 50S and 150S and reflecting probably the orebody. In agreement with the results of the borehole G25 which passes through the section 125S along east-west direction, a low resistivity zone seen between the stations 0W and 150W at a depth of about 150m may correspond to part of the orebody.

3-5-2 Daris Area

(1) Survey Location

A TEM survey consisting of two large fixed loops was carried in the central part of Daris area in order to investigate the IP anomalies detected by the TDIP survey carried out during 1996 field season.

Fig. II-3-14 includes also the location of the two large loops surveyed in Daris during this 1997 field survey.

(2) Results

Loop 1

The Figs. II-3-15 (1) and (2) show the contour maps of the TEM responses obtained in each of the 20 channels.

High TEM response values are seen in the north part of the loop within the channels 10 to 20. Within this area, a rather high response is seen around the station 500W1100W.

To confirm this anomaly, the borehole D5 was drilled, but it intersected only disseminated pyrite.

Loop 2

The Figs. II-3-16(1) and (2) show the contour maps of the TEM responses for each of the 20 channels. Somewhat high TEM responses are seen distributed to the south and south west parts of this loop. They are seen in almost every channel but specially clear in the channels from 1 to 10 where a conductor at shallow depth is assumed distributed to the south of the loop. However, the TEM response becomes weaker after the channel 15, for which it can be inferred a very low possibility of detecting massive sulphide in this zone.

3-5-3 Doqal Area

(1) Loop Locations

As a result of the IP anomalies detected during the field seasons of 1996 and 1997, a TEM survey was carried to check these anomalies but specially the metal factor distributions above 20 detected in the

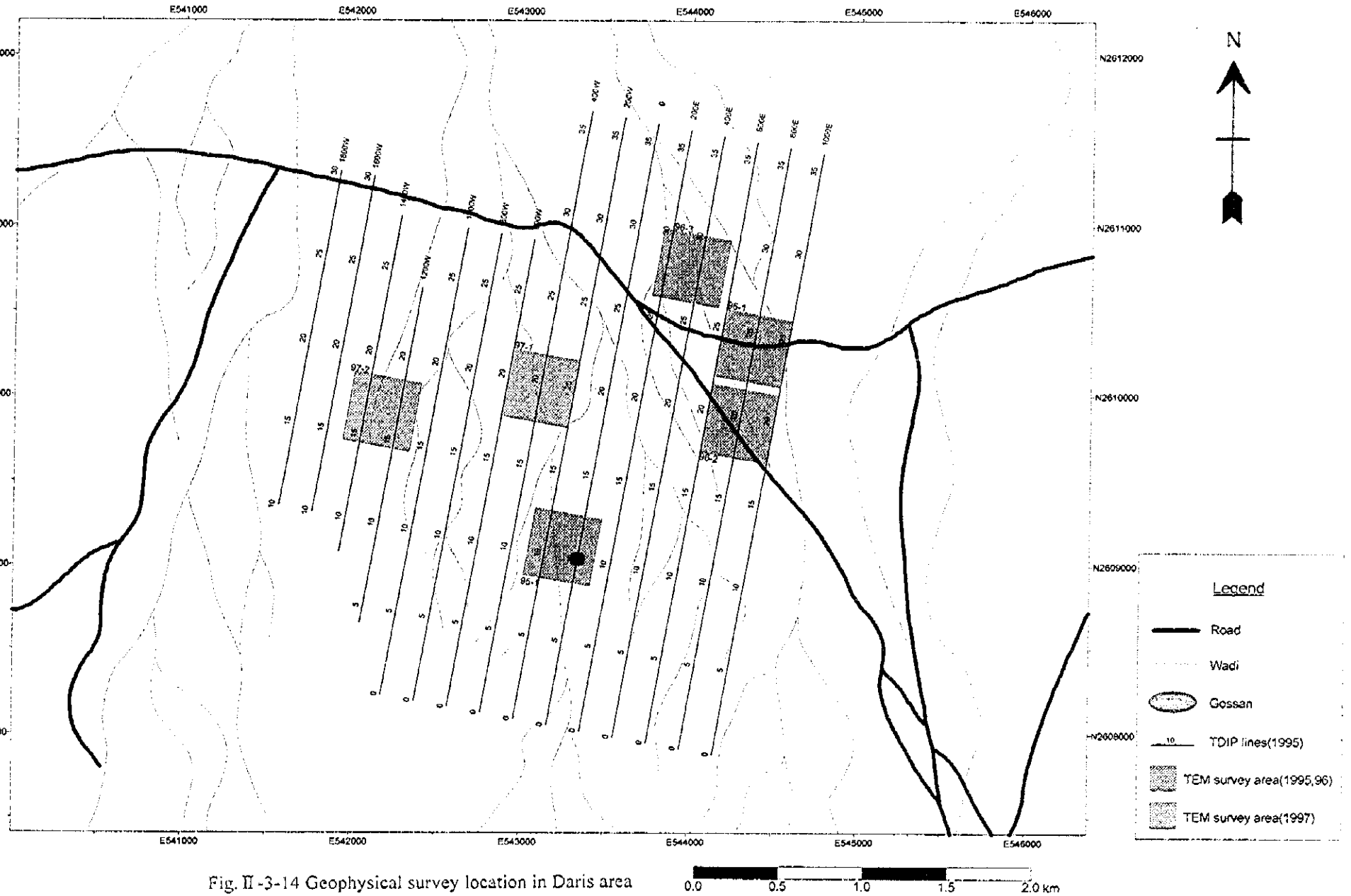

Fig. II -3-14 Geophysical survey location in Daris area